Electric bus fleet composition and scheduling

Şule Yıldırım[a], Barış Yıldız[a]

[a]*Department of Industrial Engineering, Koç University, Istanbul, Turkey*

Abstract

The low energy density of batteries and the long recharging times constitute a significant barrier for electrification of public transportation (PT) systems since electric buses (EB) require too heavy and expensive batteries to achieve the operational availability of their combustion engine counterparts. New recharging technologies such as fast chargers and dynamic wireless power transfer (DWPT) emerge as promising solutions to overcome these challenges. Optimizing the bus fleet composition and the schedules is essential to take advantage of these emerging technologies and achieve electrification of PT in a cost-efficient way. To address this challenge, this paper proposes an integer (binary) programming formulation to find the optimal electric bus fleet composition and scheduling that minimizes the total procurement cost of the buses and the operating cost of the schedules. A column generation (CG) approach is devised to obtain provably high-quality solutions, for large problem instances. The success of the approach is due to a novel dynamic programming algorithm we develop to solve the generalized resource-constrained shortest path problem that needs to be solved in each CG iterations to find out new schedules to include in the model. Extensive computational studies on large real-world PT networks attest to the efficacy of the suggested methodology and reveal valuable managerial insights from a system-wide perspective.

Keywords: Electrification of public transit, electric buses, dynamic wireless power transfer, column generation, dynamic programming, generalized resource-constrained shortest path problem

1. Introduction

The electrification trend in transportation accelerates with the recent advances in technology and rising concerns over fossil fuel usage. Similarly, in all parts of the world, public transportation (PT) is promoted as an effective tool to reduce the negative externalities of transportation such as congestion, pollution, and accidents. In the junction of these emerging trends are the electric buses (EB), which offer novel opportunities for city dwellers to have cleaner, quieter, and, most importantly, more livable cities through reduced emissions and noise. With the help of EBs, it is possible to extend the PT coverage and service quality without increasing or even reducing the carbon footprint (Quarles and Kockelman, 2018). As such, the interest in EBs is rapidly growing, and the global EB market is expected to reach the value of $215 billion, by 2026, after going through a compound annual growth rate of 26.1% during the 2020-2026 period (Globe Newswire, 2020).

Besides the growing interest, there are also significant challenges to overcome for the electrification of the PT systems in a cost-efficient way. The main challenge for EBs, as well as electric vehicles in general, is the low energy density of batteries (Li and Mi, 2014). The energy density of a battery is 88 $wh.kg^{-1}$ (Majeau-Bettez et al., 2011) while the energy density of diesel fuel is 199,550 Btu/gal (Alternative

Fuels Data Center, 2014), which is around 37.13 $kWh.kg^{-1}$. Due to this enormous density difference, pure EBs require too heavy and expensive batteries to achieve the range and the operational availability of a diesel vehicle, which is a significant obstacle for the prevalent use of EBs in PT networks. To eliminate this barrier, new recharging technologies, such as level-3 fast charging and dynamic wireless power transfer (DWPT), which enables vehicles to charge on the move, have been proposed to extend operational availability of EBs at a lower cost than increasing their battery sizes (Fuller, 2016). Such a promising opportunity has been the focus of many projects, such as On-Line Electric Vehicle (OLEV)(`www.olev.kaist.ac.kr`), SELECT (`www.select.usu.edu`), and FABRIC (`www.fabric-project.eu`).

There is a broad literature on the technical engineering challenges posed by wireless charging, but research on operations and system design issues is still emerging (Jang, 2018). In particular, optimizing the bus fleet composition and schedules comes into prominence to take advantage of the novel recharging technologies (i.e., wireless and fast charging) and benefit from the advantages of EBs at a lower cost. Considering the size of the investment to procure the EB fleets (typically reaching billions of dollars) for large PT networks, developing efficient methodologies to optimize EB fleets can provide significant savings. Besides their economic importance, such savings can bend the trend more in favor of electrified public transit with all the obvious sustainability benefits for the city residents.

Due to the extra complications introduced by the recharging needs of the EBs, existing studies on bus fleet composition and scheduling for conventional buses cannot address this urgent problem. Determining the optimal battery sizes together with the vehicles' schedules by reflecting on the complex trade-offs between the range, procurement cost, utilization, and per-mile energy usage introduces novel computational challenges that have not been adequately addressed in the literature. To address this significant gap in the literature, this study introduces the EB fleet composition and scheduling problem with fast-charging and DWPT infrastructure (EBFCS) to the literature and develops an efficient methodology to solve large size real-world instances. We propose an integer (binary) programming (IP) formulation to model EBFCS and device a column generation (CG) approach to obtain provably high-quality solutions. The success of the approach is due to a novel Dynamic Programming (DP) algorithm we develop to solve the generalized resource-constrained shortest path problems (GRSP) that need to be solved in each CG iteration to find out new schedules to include in our model. Taking advantage of the special properties of the graph structure over which we define the problem, DP can solve the GRSP instances we encounter in the CG iterations in pseudo-polynomial time.

To analyze the system-wide benefits of EBs under various charging infrastructure configurations, we study two large PT networks from Istanbul, Turkey, with orthogonal properties regarding the trip frequencies, amount of road segments shared by different lines, expected number of passengers on a typical trip, and the size of buses used. The Bus Rapid Transit (BRT) network we study in this paper, Metrobus, is a 50.7 km long route operated with long (18-25 meter) busses on dedicated lanes. Conducting more than 6,400 trips on a weekday, Metrobus is one of the main means of transportation in the city used by more than one million passengers on a typical day. Indeed, electrification of the Metrobus system is on the agenda of Istanbul Electricity, Tramway and Tunnel General Management (IETT). The second PT network we consider, the Hacıosman network, has a classical hub-and-spoke structure. Hacıosman, the

hub, is the last station of a heavily used subway line in Istanbul, and it is the starting point of 14 public transit lines carrying passengers between the subway and different districts. On a weekday, 846 trips are operated on this network by typical 12-meter buses. In an extensive computational study, we investigate the impacts of electrification of fleets, changing DWPT pickup power, extending DWPT infrastructure coverage, and improving the fast charging power transfer levels on the characterization of the resulting bus fleet and the total cost incurred to procure the fleet and operate the resulting schedules. Results of these experiments attest to the efficacy of the solution approach we develop to solve EBFCS and provide critical managerial insights for PT authorities and technology developers.

1.1. State of the art

The problem we study in this paper falls in the broader class of Transit Planning Problems (TPP) or more specifically Multi Depot Vehicle Scheduling Problems (MDVSP). For the wast literature on the topic, we refer interested reader to comprehensive reviews by Guihaire and Hao (2008) and by Erdelić and Carić (2019). Here, we focus on recent studies involving settings similar to the ones we consider or involving methodologies similar to the ones we use.

TPP covers all the problems that should be addressed to design a PT system from scratch. Ideally, all the issues regarding TPP should be addressed at once to archive the "perfect" plan. However, it is not possible to do so due to computational intractability, and TPP is solved in five recurring and consecutive steps: (1) network design, (2) setting of frequencies, (3) timetabling, (4) vehicle scheduling and (5) crew scheduling and rostering (Ceder and Wilson, 1986). In this study, we focus on the fourth step, which is an extensively studied research area in the last 60 years. Ibarra-Rojas et al. (2015) review vehicle scheduling (VS) problems in five categories: single-depot VS, multi-depot VS, robust VS, dynamic VS and vehicle rescheduling. This paper extends MDVSP for EBs considering a recharging infrastructure composed of fast-charging and DWPT technologies. MDVSP is proven to be NP-hard by Bertossi et al. (1987). Therefore EBFCS is also an NP-hard problem, as it generalizes MDVSP. Similar to our study, column generation (CG) based methodologies are widely used to solve MDVSP and its extensions. In their seminal paper, Ribeiro and Soumis (1994) formulate MDVSP as a set partitioning problem and suggest a CG approach to solve its linear relaxation. Showing that the LP relaxation solutions provide tight lower bounds for the integer program, their study motivated various researchers to use similar formulations and develop CG-based solution approaches to solve various extensions of MDVSP. Examples include MDVSP with time windows (Desaulniers et al., 1998), heterogeneous fleets (Taillard, 1999; Guedes and Borenstein, 2015, 2018), inter-depot routes (Muter et al., 2014), controlled trip shifting (Desfontaines and Desaulniers, 2018), and fast-charging (van Kooten Niekerk et al., 2017). We also formulate EBFCS as a set partitioning problem and solve it with a CG-based approach. However, unlike the aforementioned studies, the pricing problem we have to deal with is not an RSP. Due to the complex energy (electric charge) loss and gain dynamics imposed by a recharging infrastructure that has both plug-in fast-charging and DWPT capabilities, we need to solve a generalization of RSP (GRSP) for which we devise a new DP algorithm.

As a well-known NP-Hard problem, RSP emerges as the pricing problem in many CG-based algorithms for various vehicle routing and scheduling problems, and there is a wide literature on different algorithmic approaches to solve it (Di Puglia Pugliese and Guerriero, 2013). One of the most used algorithms to solve large RSP instances is the Pulse Algorithm (PA) by Lozano and Medaglia (2013). The intuition behind PA is to propagate pulses through a network and form a feasible path whenever a pulse starting from the source node reaches the sink node. In the worst case, the algorithm may enumerate all the feasible paths by requiring a high computational effort, and the success of the algorithm is due to the aggressive pruning strategies to prevent the propagation of pulses without eliminating the optimal path. In a recent study, Cabrera et al. (2020) extended PA by a bidirectional search strategy which propagates the pulses from both source and sink nodes. In the worst case, the algorithm enumerates all the feasible paths twice, once starting from the source and once starting from the sink. The efficiency of the suggested methodology in practice is due to the effective pruning strategies that are enabled by the bidirectional search approach. The modified PA can find the optimal solution on real-road networks with up to 6 million nodes and 15 million arcs. Thomas et al. (2019) also consider a bidirectional search approach to solve RSP. Researchers show that although their bidirectional $A^\star$ algorithm performs poorly on loosely constrained problems, it can outperform unidirectional $A^\star$ methods and compete with and sometimes outperform the best-known algorithms when the constraints are more binding. Another advantage of the suggested approach is using less memory, which helps find the optimal solution in large networks. Although existing approaches so far have been very efficient by using fathoming rules on an implicit enumeration (Aneja et al., 1983) or by using Dual Lagrangean Problem for an improved fathoming (Mehlhorn and Ziegelmann, 2000; Dumitrescu and Boland, 2003), considering negative resource consumption invalidates most of the pruning strategies and makes these approaches impracticable for EBFCS . To address this issue and taking advantage of the special structure of the GRSP we deal with, we extend current literature on RSP solutions and suggest a pseudo-polynomial time algorithm to solve the GRSP instances we encounter in our CG iterations.

Fueled by the rising interest in electrification in PT, the literature on EB fleet scheduling (EBFCS) is rapidly expanding. The existing literature can be classified by the recharging technology considered. Earlier work on EBFCS focuses on the battery swap technologies, which decouples public transit and recharging operations, as EBs can continue their service while the batteries are charged independently in such settings (CHA, 2013; Kim et al., 2015). At the strategic level, the cost-effective placing of charging infrastructure and battery sizing are the two main decisions investigated in this context (Kunith et al., 2017; Li et al., 2018). At the operational level, management of recharging loads in the swap stations is the primary concern to avoid disruptions in the PT service (Dai et al., 2014). In this study, our focus is on the fast-charging and DWPT technologies where recharging is an essential part of the vehicle schedules. Sassi and Oulamara (2017) is among the earliest studies that consider plug-in charging infrastructure to support PT operations. The authors assume a mixed fleet of combustion engine and electric buses and propose an IP formulation that aims to maximize the total weight of tours processed by EBs and minimize the charging costs. Assuming a single depot and vehicle type van Kooten Niekerk et al. (2017) develops a CG-based heuristic to solve real-world problem instances from the city of Leuven. Janovec and Kohání (2019) uses an exact linear programming approach to solve EBFCS by considering partial charging, charging at

multiple locations, and time continuity. Approaching the problem from an operational level, Tang et al. (2019) study the robust EBFCS to avoid service disruptions due to stochastic urban traffic conditions that impact travel times and energy consumption. In a recent study, Zhou et al. (2020) develop a Multi-objective Bi-level programming model to collaboratively optimize the vehicle scheduling and charging scheduling of the mixed bus fleet under the operating conditions of a single depot. An (2020) focus on the recharging facility location problem and propose a stochastic integer programming formulation to jointly solve the EB scheduling and infrastructure design problems, under recharging demand uncertainty. Focusing solely on the fast-charging technology, the aforementioned studies do not consider the use of DWPT and fleet composition (battery sizing) decisions.

There is extensive literature on the design of DWPT technology for EV charging (Mou et al., 2019), whereas the literature on operations and systems issues is still emerging. Since the technology is recently commercialized by KAIST, there are many questions waiting to be answered. Studies especially focus on areas such as charging infrastructure design, driving range extension analysis, cost-benefit analysis, environmental analysis, and supporting systems (Jang, 2018). The first three of those areas are the ones that inspired us to focus on EBFCS . Concentrating on the initial design of DWPT network on urban transportation, Liu et al. (2017) developed a MIP model to optimize the battery sizes of an EB fleet and the allocation of DWPT facilities on a DWPT electric bus system and Liu and Song (2017) extended the model to solve a robust problem. A study by Helber et al. (2018) focuses on designing another type of DWPT network for electric apron vehicles by taking into account airline transport operations. The main objective of the study is to locate inductive transmitter and power supply units within the side road network of an airport. From a managerial perspective, Bi et al. (2017) show, depending on the parameters, wireless charging EBs can be more economical than conventional diesel, diesel hybrid, and plug-in charging electric buses. The novel opportunities offered by DWPT for commercial fleets and public transit systems have been the focus of several studies, like ours. Chen et al. (2017) find out that DWPT should be used initially for commercial fleet vehicles having a higher value of time. Stamati and Bauer (2013) use a simulation approach to show 500 km range is achievable by a 24kWh battery, using 25kWh pick-up power and 40% DWPT infrastructure coverage, indicating the considerable potential of the technology to offer significant costs savings for the electrification of public transit networks. Bi et al. (2015) compare the required battery sizes for DWPT and plug-in charging and find out that the battery size can be reduced by one-third if DWPT is used. A case study conducted by Fuller (2016) shows that even if the battery cost falls to $100 per kWh, DWPT can extend the vehicle range at a lower cost than increasing the battery size. Therefore, even if the battery costs fall, DWPT will still be an attractive technology. Although all the aforementioned studies present powerful insights about the potential benefits of DWPT for reducing the costs of using EBs in PT networks, to the best of our knowledge, our study is the first one to investigate those claims on large size real-world systems, considering the interactions between all the important aspects of the technology, such as DWPT pick-up power and network coverage, fast charging (level-3) capabilities, PT network topologies, and energy consumption rates of the buses, which do not only depend on the size of the batteries but are also impacted by the operational conditions such as the trip speed profiles and vehicle loads that can change during the day.

1.2. Contributions and organization of the paper

With respect to the existing literature, the contributions of this study can be summarized as follows.

- Introducing EBFCS to the literature, this study is the first one to jointly consider multiple depots, multiple vehicle types (battery sizing decisions), and multiple recharging technologies together to find the optimal EB fleet configuration that can serve a given set of PT trips with the minimum total procurement and operating costs.

- We develop an efficient CG-based algorithm that can provide provably high-quality solutions of EBFCS for large-size real-world problems with thousands of PT trips, to be served by hundreds of EBs with varying battery capacities. The computational efficiency of the approach is due to a new DP algorithm we develop to solve the generalized resource-constrained shortest path problem that needs to be solved in CG iterations to find new schedules to include in the model.

- We conduct extensive numerical experiments on two large real-world PT networks with orthogonal properties in critical problem parameters to analyze the system-wide benefits of EBs. Providing important managerial insights, our results shed light on critical interactions between the optimal fleet composition and the structure and the energy transfer capabilities of the recharging infrastructure. In particular, our results show that:

  - Although electrification increases the number of required buses that are already more expensive than their combustion engine counterparts, it still reduces the total cost incurred (up to 43% in our experiments) due to the low operational cost (electricity and maintenance) for the current market parameters.
  - DWPT can play a critical role in enhancing the benefits of electrification by extending operational availability of the EBs, which in turn reduces the size of the EB fleets (more than 20% in our experiments), and reducing the required battery sizes (more than 53% in our experiments). To reap the full benefits of the technology, certain power transfer rates are should be achieved (pick-up powers beyond 60kWh might be desired), especially when a small percentage of the road segments would have the DWPT capabilities.
  - Increasing the fast charging power can provide significant cost reductions, but the marginal benefit of higher charging powers drops drastically after a threshold (i.e., beyond 120kWh in our experiments).

The rest of the paper is organized as follows. Section 2 presents the formal definition of EBFCS and the details of the solution approach we develop to solve it. In Section 3, we present the results of our numerical experiments and discuss the important insights we derive from them. Finally, we conclude in Section 4 with some final remarks.

2. Mathematical model

2.1. Notation and problem definition

This section presents definitions and notation pertinent throughout the paper. Additional definitions and notation will be listed as needed.

Let L be the set of public transit lines that are to be operated by EBs. Each line $\ell \in L$ is characterized by a sequence of time scheduled trips T_ℓ, which visit the same sequence of bus stops at different times of the day. We define T as the set of all the trips that will be operated by an EB, i.e., $T = \cup_{\ell \in L} T_\ell$. The trip set is a problem parameter in EBSFC predetermined by the PT authorities, considering the passenger demand and target service quality. The set of available EB configurations is denoted by B, where each bus type $b \in B$ has a different battery size β_b and purchasing cost c_b. The set of depots, which are typically the first and/or the last bus stop in a trip and have required space, services, and amenities to park and replenish (recharge) the buses when they are not in service, are denoted by D. We assume that all the depots are equipped with fast charging infrastructure where the fast charger power transfer level is denoted by ψ_f, and the number of fast chargers at a depot is large enough to charge all the buses parked there at any given time. We assume that EBs are fully charged overnight (i.e., EBs start with full charge, at the beginning of the day).

The sequence of bus stops that are visited by a trip $t \in T$ is denoted by K_t, where the first and last bus stops are indicated as o_t and d_t. To capture the dynamism of the network (changing traffic conditions, speed profiles, the number of passengers on the busses, etc.), and reflect its effects on the associated parameters, we assume that a bus stop is used only by a single trip (i.e., a different copy of the same physical bus stop is generated for each trip that uses it). Each trip t has a predefined path that visits all its bus stops K_t, following the sequence of road segments R_t, where each road segment is a stretch of the physical road on which all the important parameters that impact the energy usage/gain of an EB (e.g., slope, friction, availability of DWPT and the pick-up power) remains the same. Similar to the bus stops, we assume that each road segment is used only by a single trip (i.e., a different copy of the same physical road segment is generated for each trip that uses it). Clearly, defining bus stops and road segments uniquely, one can represent a trip either by its list of bus stops or by its list of road segments. We avoid such a simplification and define the problem parameters (data) more straightforwardly. The first and last road segments of a sequence R_t, $t \in T$, are indicated by $\bar{r}_t$ and $\underline{r}_t$, respectively. For each trip $t \in T$, the successor of road segment $r \in R_t \setminus \{\underline{r}_t\}$, is denoted by $\tilde{r}$. The time table of a trip t specifies the time when a bus stop $k \in K_t$ will be visited during the trip, which we denote as θ_k. Timetables are planned by PT authorities taking important system dynamics into account, such as expected traffic conditions that impact vehicle speeds on the road segments and passenger demand that impact dwell times at bus stops. Implied by the timetables and typical of public transit operations, trips have known speed profiles on the road segments that govern the movements of the buses on the road segments. The amount of time that it takes for an EB to travel on a road segment $r_t \in R_t$ on a trip $t \in T$ is denoted by α_{r_t}.

Considering the technical specifications of the bus (weight, powertrain technology, etc.), operational

conditions of the trip (traffic conditions, number of onboard passengers, etc.) and the physical condition of the road segment (slope, friction, availability of DWPT and the pick-up power, etc.), the amount of energy spent by a type b bus, on a trip $t \in T$, to travel on a road segment $r \in R_t$, is given as $\underline{\kappa}^b_r$. EBs can also gain energy by traveling on road segments with DPWT capability where the pick-up power is denoted by ψ_w. The amount of energy gained by a bus of type b, in a trip $t \in T$, on a road segment $r \in R_t$ is denoted by $\hat{\kappa}^b_r$. To simply the notation, we define the net energy consumption of a type $b \in B$ bus, on a trip $t \in T$, on a road segment $r \in R_t$ as $\kappa^b_{tr} = \underline{\kappa}^b_{tr} - \hat{\kappa}^b_{tr}$, where the negative values indicate that the bus gains energy on the road.

We say a trip $j \in T$ is an *admissible successor* of a trip $i \in T \setminus \{j\}$, if it is possible for a bus to first complete the trip i and then continue with the trip j, i.e., the bus can reach at the bus stop o_j before $\theta^{o_j}_j$, when it departs from d_i at time θ_{d_i}. The set of all admissible successors of a trip $i \in T$ are denoted by $\bar{T}_i$. In other words, the set of admissible successors of trip i is the set of alternative trips that can be operated by a bus after completing the trip i, assuming that the remaining battery is sufficient. As will be clear once we introduce the details of our solution approach, these sets play an important role in the DP algorithm by indicating the set of actions that can be taken by a bus after completing a trip. Also, we want to highlight that we allow a bus to serve multiple lines, which is preferred/implemented by many PT managements across the globe to improve vehicle utilizations. Although serving multiple lines with a bus may introduce additional difficulties in planning and operating a schedule, economic benefits due to the reduced number of buses needed in the system usually out-weights such disadvantages, especially when there are several lines in the network with low trip frequencies. However, if PT management prefers to use a bus only on a single line, or on a group of lines, such restrictions can be easily imposed in our model. To do that, one can simply modify the definition of admissible successors of a trip, which essentially decomposes EBFCS into independent sub-problems for each line or line group.

Between a trip $i \in T$ and any of its admissible successors $j \in \bar{T}_i$ there is a predefined *transition path* p_{ij} which indicates the sequence of road segments R_{ij} to travel from d_i to o_j and the amount of time to travel each road segment $r \in R_{ij}$. There can be several alternative paths to follow while transitioning from a trip i to j and the mathematical definitions of these paths may differ based on the objective. For example, one may choose the path that takes the least time to increase operational availability or the path that spends the least energy to reduce the energy cost. Among such alternatives, in our study we define transition paths as the fastest path from the last bus stop in i to the closest depot to the first bus stop of the trip j (i.e., the path that has the maximum recharging time at the depot closest to the first bus stop of the trip j). The energy consumed for a re-positioning bus of type $b \in B$, on a road segment $r \in R_{ij}$ for some $i \in T$ and $j \in \bar{T}_i$, is denoted by $\underline{\kappa}^b_{ijr}$ and the net energy gain/loss for a re-positioning bus of type $b \in B$, on a road segment $r \in R_{ij}$ for some $i \in T$ and $j \in \bar{T}_i$, is denoted by κ^b_{ijr}. If a transition path $p_{ij}, i \in T, j \in \bar{T}_i$ visits a depot $\delta \in D$, an artificial road segment r_δ is added in the sequence R_{ij} to represent the parking of the bus in the depot for α_{r_d} hours. If the parking time is longer than a threshold ψ, which can be defined according to the operational conditions required to position the bus, the EB can use that time to recharge its batteries as much as the time spent at the depot permits. For the sake of simplicity, we assume that the transition paths are planned such that the EBs have the maximum parking time at the closest depot

to the first stop of the following trip. For the fast charging at depots, the amount of energy gained by a type $b \in B$ bus with p percent full batteries after an $\alpha \geq 0$ hours of recharging is given by $f(b, p, \alpha)$. Clearly, the exact form of the *recharging function* $f : B \times [0, 1] \times \mathbb{R}_+ \to \mathbb{R}_+$ is determined by the technical specifications of the EB and the recharging infrastructure (Yee et al., 2014). For the modeling reasons that will be clear when we introduce our solution approach in the next subsection, for each road segment $r \in \{\cup_t R_t\} \cup \{\cup_{i \in T, j \in \bar{T}_i} R_{ij}\}$ and a bus type $b \in B$ we define an energy loss function $\rho_r^b : \mathbb{R}_+ \to \mathbb{R}$ of the following form.

$$\rho_r^b(\gamma) = \begin{cases} -f(b, \gamma, \alpha_r), & \text{if } r \text{ represents the parking in a depot} \\ \kappa_r^b, & \text{otherwise} \end{cases} \tag{1}$$

where $\gamma \geq 0$ is the SOC when the EB starts traveling on the road segment r.

A *bus schedule* σ is a sequence of trips $\tau_\sigma = \{t_1^\sigma, \ldots, t_{n_\sigma}^\sigma\}$ that are to be operated with an EB of type $b_\sigma \in B$. The EB that will execute a schedule σ starts its day from the *start depot* $\delta_{t_1^\sigma}$, which is the depot with the shortest distance to the first stop of the first trip t_1^σ, and follows the sequence of road segments indicated by the *start path* $p_{t_1^\sigma}$ to reach at $o_{t_1^\sigma}$. Similarly, when finishing their schedules EBs move to their *exit depot* $\delta_{t_{n_\sigma}^\sigma}$ with the shortest distance to the last bus stop $d_{t_{n_\sigma}^\sigma}$, following the *exit path* $\bar{p}_{t_{n_\sigma}^\sigma}$. Clearly, the start and the final depots of a schedule do not have to be the same, and we assume that the EBs can be repositioned during their off times (typically at night) to repeat their schedules the next day, if needed. We also want to note that, our solution approach does not depend on considering the shortest distance to determine start and exit depots/paths. It can also work if one would prefer other criteria, such as looking for the paths with the least energy usage, although in many cases, the result would be the same.

A schedule σ is called *feasible* if there are possible transitions between its trips (i.e., $t_{i+1} \in T_i$ for all $i = 1, \ldots, n_\sigma - 1$) and starting with a full charged battery, EB's state of charge (SOC) never goes beyond the range $[\epsilon_{b_\sigma}^{min}, \epsilon_{b_\sigma}^{max}]$ where $0 \leq \epsilon_{b_\sigma}^{min} \leq \epsilon_{b_\sigma}^{max} \leq 1$. The set of all feasible bus schedules is denoted by S. Considering the associated bus type b_σ, the cost c_σ of a schedule $\sigma \in S$ is defined as the sum of the purchase cost of a type b_σ bus and the operational cost incurred to complete the trips and required transitions in the schedule which is composed of electricity and maintenance costs in our case.We omit the labor costs in this calculation because it is not a differentiating factor when alternative vehicle technologies and recharging infrastructure structures are considered. Moreover, bus drivers usually earn fixed salaries, and their daily driving hours are mainly determined/restricted by government regulations and union agreements. In line with the existing literature, in this study, we focus on the fleet composition and scheduling problem and defer the solution of the crew scheduling problem to a separate study.

As a quick reference, we present the outline of the mathematical notation in Table 5 and formally define EBFCS as follows.

Definition 1. *Given a set of lines L to operate with EBs, the set of alternative EB types B, the set of depots D and road segments R; Electric Bus Fleet Composition and Scheduling Problem (EBFCS) is to find minimum cost exact cover $S^* \subset S$ for the trip set $T = \cup_{\ell \in L} T_\ell$.*

Table 1: Outline of notation

Indices:	
l:	Line
b:	Bus type
t:	Trip
k:	Bus stop
r:	Road segment
σ:	Schedule
δ:	Depot
Sets:	
L:	Set of public transit lines
B:	Set of available EB configurations (types)
T:	Set of all public transit trips
R:	Set of road segments
D:	Set of depots
S:	Set of feasible schedules
T_ℓ:	Set of scheduled trips defining a line $\ell \in L$
K_t:	Sequence of bus stops that are visited by a trip $t \in T$
R_t:	Sequence of road segments that a trip $t \in T$ follows
$R_{\bar{t}t}$:	Sequence of road segments to be traveled to traverse between trips $\bar{t} \in \bar{T}_t$ and $t \in T$
$\bar{T}_t$:	Set of all admissible successors of a trip $t \in T$
Parameters:	
β_b:	Battery size of a type $b \in B$ bus
c_b:	Purchasing cost of bus type $b \in B$
o_t:	The first bus stop visited by a trip $t \in T$
d_t:	The last bus stop visited by a trip $t \in T$
$\bar{r}_t$:	The first road segment of a sequence $R_t, t \in T$
$\underline{r}_t$:	The last road segment of a sequence $R_t, t \in T$
$\tilde{r}_t$:	Predecessor of road segment r_t in a sequence $R_t, t \in T$
θ_k:	Time when a bus stop $k \in K_t$ will be visited in a trip $t \in T$
α_{r_t}:	Amount of time that it takes for an EB to travel on a road segment $r_t \in R_t$ on a trip $t \in T$
ψ_f:	Fast charger power
p_{ij}:	Transition path which indicates the sequence of road segments R_{ij} to travel from d_i to o_j
$\underline{\kappa}^b_{ijr}$:	Energy consumed for re-positioning a $b \in B$ tyoe bus, on a road segment $r \in R_{ij}$ for some $i \in T$ and $j \in \bar{T}_i$
κ^b_{ijr} :	Net energy gain/loss for re-positioning a $b \in B$ type bus, on a road segment $r \in R_{ij}$ for some $i \in T$ and $j \in \bar{T}_i$
r_δ:	An artificial road segment representing the parking of the bus in the depot depot $\delta \in D$ for α_{r_d} hours
$\underline{\kappa}^b_{tr}$:	Amount of energy spend by a type b bus, in a trip $t \in T$, on a road segment $r \in R_t$
$\hat{\kappa}^b_{tr}$:	Amount of energy gained by a type b bus,in a trip $t \in T$, on a road segment $r \in R$
κ^b_{tr}:	Net energy consumption of a type $b \in B$ bus, on a trip $t \in T$, on a road segment $r \in R_t$
$\delta_{t^\sigma_1}$:	Start depot with the shortest distance to the first stop of the first trip t^σ_1
$p_{t^\sigma_1}$:	Start path followed to reach at $o_{t^\sigma_1}$
$\delta_{t^\sigma_{n_\sigma}}$:	Exit depot with the shortest distance to the last bus stop $d_{t^\sigma_{n_\sigma}}$
$\bar{p}_{t^\sigma_{n_\sigma}}$:	Exit path followed from the last bus stop $d_{t^\sigma_{n_\sigma}}$
c_σ:	Cost of operating schedule $\sigma \in S$
Variables	
x_σ:	Binary variable to indicate whether schedule $\sigma \in S$ is operated

2.2. Mathematical formulation

Our formulation builds upon the set of feasible bus schedules. Defining $S(t)$ as the set of feasible schedules that trip $t \in T$ is included in and considering the binary assignment decisions x_σ, which indicate whether a schedule $\sigma \in S$ is to be operated or not, we define our binary programming model P as follows.

$$\min \sum_{\sigma \in S} c_\sigma x_\sigma \tag{2}$$

$$s.t. \quad \sum_{\sigma \in S(t)} x_\sigma = 1 \quad \forall t \in T \tag{3}$$

$$x_\sigma \in \{0,1\} \quad \forall \sigma \in S \tag{4}$$

The objective (2) is to minimize the total cost of operating schedules, and the constraints (3) make sure that an exact cover is formed. Constraints (4) define the domain of the decision variables. Here we want to note that, for the sake of simplicity, we did not consider the passenger capacities of the buses in the definition of the feasible schedules. However, if the expected number of passengers in a trip requires a particular bus type, this can be easily incorporated into our model by updating the definition of the feasible schedules to include this restriction. In that case, for a trip $t \in T$ the set S_t would only include those schedules that match the bus type requirement of the trip.

Considering the use of feasible schedules as decision variables, the formulation P can address complex energy consumption, gain, and storage dynamics of the EBs and their interactions with the operational conditions of the considered PT trips, without imposing any simplifying assumptions. Although such an approach enables us to formulate EBFCS with a straightforward linear model, the computational difficulties to generate and include the exponentially many feasible schedules require developing advanced methodologies to solve it for large problem instances. For that purpose, we develop a column generation approach (CG) that first solves the linear relaxation of P, and then obtains provably high-quality solutions by taking advantage of the small linear relaxation gaps and solving the P by with those schedules generated in the CG phase and IP-friendly columns that are generated by a heuristic column generation method that will be explained in the sequence.

2.2.1. Linear relaxation solution

Let LP be the linear relaxation of the binary programming formulation P, which we obtain by replacing the Constraints (4) with the following.

$$x_\sigma \geq 0 \quad \forall \sigma \in S. \tag{5}$$

Here we want to note that the constraints $x_\sigma \leq 1, \forall \sigma \in S$ are redundant, and hence not included in LP, because operating the same schedule more than once already violates constraints (3).

To solve LP, we start with a small subset of feasible schedules (i.e., with a restricted formulation) and iteratively generate new ones as needed. A basic approach for generating initial columns is explained in Appendix A. At each iteration of the CG algorithm, we solve a *pricing problem* to identify feasible bus schedules that are not in the restricted formulation but have a favorable reduced cost or conclude that there are no such schedules, and the procedure can be terminated. Let LP^k be the restricted LP formulation in the k^{th} iteration of the CG algorithm. The set of feasible schedules included in P^k is

denoted by X^k. Let u^k be the vector of dual variables associated with constraint (3) for the restricted problem P^k. Then the reduced cost ζ_σ of schedule variable x_σ can be calculated as follows.

$$\zeta_\sigma = c_\sigma - \sum_{t \in \tau_\sigma} u_t. \tag{6}$$

Note that solving the pricing problem is equivalent to finding the feasible schedule σ^* with the smallest reduced cost. If $\zeta_{\sigma^*} < 0$, we add σ^* to the restricted problem and move to the next iteration of the CG algorithm. Otherwise, we declare the solution of the restricted problem as optimal and stop the algorithm. Before presenting the details of the solution approaches we consider to solve the pricing problem, we first define the generalized resource constraint shortest path problem (GRSP) that generalizes RSP by considering negative resource consumption (i.e., resource gains) and the resource storage capacity limitations. We then show that one can solve the pricing problem by solving a GRSP problem for each bus type $b \in B$.

Definition 2. *Let $G(N, A)$ be a directed graph, where each arc $a \in A$ has an associated cost $c_a \in \mathbb{R}$, and a resource function $\rho_a : \mathbb{Z}_+ \to \mathbb{R}_+$, where $\rho_a(\gamma)$ indicates the amount of resource usage on the arc a when travelling it with a resource level γ. Given a source $s \in N$, a sink $t \in N$, resource storage capacity Γ and an initial resource level $\bar{\Gamma} \leq \Gamma$ the GRSP is to find a simple path from s to t (an ordered sequence of arcs) $p^* = \{p_1^* \ldots, p_k^*\}$ in G, with the smallest cost and non-negative resource levels $\lambda_i = \min\{\Gamma, \lambda_{i-1} - \rho_i(\lambda_{i-1})\} \geq 0$, for all $i = 1, \ldots, k$, where $\lambda_0 = \bar{\Gamma}$.*

For a bus type $b \in B$, we define the *pricing graph* $G_b(N_b, A_b)$, as a directed graph with the node set N_b and the arc set A_b. Besides the two special nodes: $\boldsymbol{o}$ and $\boldsymbol{d}$ to represent the start and end of a schedule, the node set contains the road segments of all the trips and the transition paths, i.e., we have $N_b = \{\boldsymbol{o}, \boldsymbol{d}\} \cup \{\cup_t R_t\} \cup \{\cup_{i \in T, j \in \bar{T}_i} R_{ij}\}$. The arc set A_b is composed of the following four groups of arcs.

- *start arcs*: Representing the start of a schedule, the set of start arcs A_b^1 is composed of the arcs $a_i = (\boldsymbol{o}, i)$ for trip $i \in T$. We define the cost of a start arc $a_i = (\boldsymbol{o}, i), i \in T$ as $c_{a_i} = c_{p_i}^b - u_i$, where $c_{p_i}^b$ is the cost of the energy that an EB of type b uses on the start path p_i. The resource usage on an arc $a_i \in A_b^1$ is defined by the constant function $\rho_a(\gamma) = \kappa_i^b, \forall \gamma \geq 0$, where κ_i^b is the net energy usage of a fully charged EB of type b for traveling the starting path p_i.

- *exit arcs*: Representing the ending of a schedule, the set of exit arcs A_b^2 is composed of the arcs $a_i = (i, \boldsymbol{d})$ for trip $i \in T$. We define the cost of an arc $a_i = (i, \boldsymbol{d}), i \in T$ as $c_{a_i} = c_{\bar{p}_i}^b$, where $c_{\bar{p}_i}^b$ is the cost of the energy that an EB of type b uses on the exit path $\bar{p}_i$. The resource usage on an arc $a_i \in A_b^1$ is defined by the constant function $\rho_a(\gamma) = \bar{\kappa}_i^b, \forall \gamma \geq 0$, where $\bar{\kappa}_i^b$ is the minimum amount of energy needed to complete the exit path $\bar{p}_i$ with a bus of type b.

- *transition arcs*: For each trip pair $(i, j), i \in T, j \in T_i$ the set of transition arcs A_b^3 include the arcs $a_{ij}^1 = (\underline{r}_i, \bar{r}_{ij})$ and $a_{ij}^2 = (\underline{r}_{ij}, \bar{r}_j)$, where $\underline{r}_i$ is the last road segment in R_i, $\bar{r}_{ij}$ is the first road segment in R_{ij}, $\underline{r}_{ij}$ is the last road segment in R_{ij} and $\bar{r}_j$ is the first road segment in R_j. For the arc a_{ij}^1 we

define the cost as $c_{a^1_{ij}} = c^b_{\bar{r}_{ij}}$ where $c^b_{\bar{r}_{ij}}$ is the cost of energy consumed to travel the road segment $\bar{r}_{ij}$, and the resource usage is defined as $\rho_{a^1_{ij}} = \rho^b_{\bar{r}_{ij}}$. For the arc a^2_{ij} the cost defined as $c_{a^2_{ij}} = c^b_{\bar{r}_j} - u_j$ and the resource usage is defined as $\rho_{a^2_{ij}} = \rho^b_{\bar{r}_j}$.

- *travel arcs*: For each road segment $r \in \cup_{i \in T} R_i \cup_{i \in T} \cup_{j \in T_i} R_{ij}$ the set of travel arcs A^4_b includes an arc $a_r = (r, \tilde{r})$, with a cost $c_{a_r} = c^b_{\tilde{r}}$ and resource usage $\rho_{a_r} = \rho^b_{\tilde{r}}$.

Figure 1 shows an example of a pricing graph for a small instance with $T = \{t_1, t_2, t_3\}$, $T_1 = \{t_3\}$, $T_2 = \{t_3\}$, $T_3 = \emptyset$ and u=$\{u_1, u_2, u_3\}$. In the arc labels, the first term indicates the cost, and the second term shows the associated resource usage function. As one can easily observe from the figure, the solution of the GRSP problem on a pricing graph G_b returns the schedule with the smallest reduced cost for an EB of type b. Laying the foundation of the solution approach we suggest for the pricing problem, we formally state this observation in the following propositions.

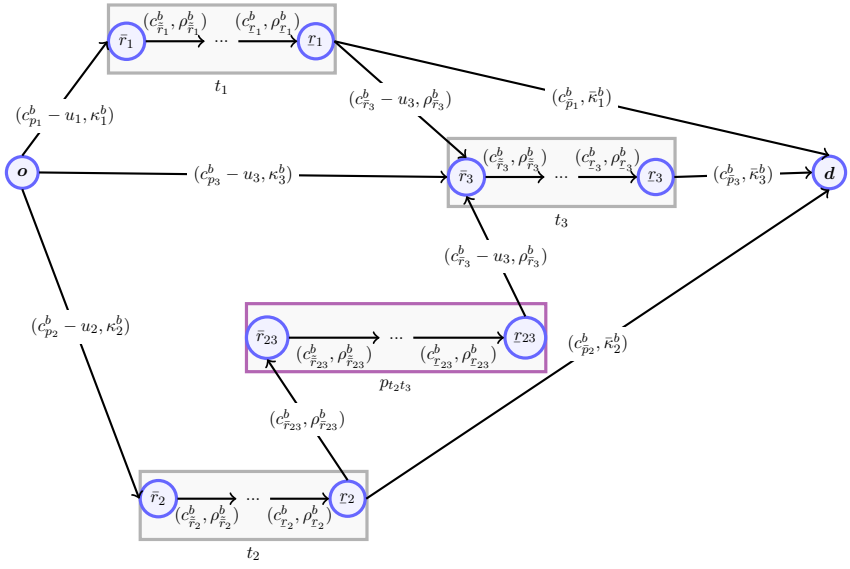


Figure 1: Example of a pricing graph

Proposition 1. *The pricing problem can be solved by solving a GRSP problems for each bus type $b \in B$.*

Proof. To prove the claim, we first show that there is a one-to-one mapping between the feasible schedules of a type b bus and the feasible solutions of the GRSP problem on the pricing graph G_b. To see this, let σ be a feasible schedule. Then the corresponding path $p_\sigma = \{d_{t^\sigma_1}, \ldots R_{t^\sigma_i}, R_{t^\sigma_i t^\sigma_{i+1}}, \ldots, R_{t^\sigma_{n_\sigma - 1}}, R_{t^\sigma_{n_\sigma - 1}, t^\sigma_{n_\sigma}}, R_{t_{n_\sigma}}, d_{t_{n_\sigma}}\}$ is a feasible solution for the GRSP problem on the graph G_{b_σ}. Similarly, if a path $p = \{d_{t_1}, \ldots, R_{t_i}, R_{t_i t_{i+1}}, \ldots, R_{t_{n-1}}, R_{t_n, t_n}, d_{t_n}\}$ is a feasible solution of the GRSP problem on the graph G_b, $b \in B$, then the schedule σ_p with the trip sequence $\tau_{\sigma_p} = \{t_1, \ldots, t_n\}$ is a *feasible schedule* for a bus type of b. The results follows from the observation that for any feasible schedule σ that is associated with a bus type b, we have $\zeta_{\sigma_p} = c_b + c_p$, where c_p is the total cost of the arcs that p include. □

We next present an IP formulation to solve the GRSP on a pricing graph G_b. For that, we first define the following decision variables:

- $y_{ij}= \begin{cases} 1, & \text{if arc } (i,j) \in A_b \text{ belongs to the path,} \\ 0, & \text{otherwise.} \end{cases}$
- $e_i \geq 0$: resource level (SOC) at node $i \in N_b$.

With these decision variables the formulation $\mathcal{P}_b$ to solve the GRSP on a given pricing graph G_b can be written as follows.

$$\min \sum_{(i,j)\in A_b} c_{ij} y_{ij} \tag{7}$$

$$\text{s.t.} \sum_{(i,j)\in A_b} y_{ij} - \sum_{(j,i)\in A_b} y_{ji} = \begin{cases} 1, \ if\ i = \boldsymbol{o}, \\ -1, \ if\ i = \boldsymbol{d} \\ 0, \ o.w. \end{cases} \qquad \forall i \in N_b \tag{8}$$

$$e_j \leq e_i - \rho_{ij}(e_i) + (1 - y_{ij})\Gamma \qquad \forall (i,j) \in A_b \tag{9}$$

$$e_{\boldsymbol{o}} = \Gamma \tag{10}$$

$$0 \leq e_i \leq \Gamma \qquad \forall i \in N_b \setminus \{\boldsymbol{o}\} \tag{11}$$

$$y_{ij} \in \{0,1\} \qquad \forall (i,j) \in A_b \tag{12}$$

The objective (7) is to minimize the cost of the path. The flow balance constraints (8) ensure that the solution provides a path from origin $\boldsymbol{o}$ to the destination $\boldsymbol{d}$. The resource balance constraints (9) enforce that the energy losses/gains are taken into account to determine the resource levels at each node on the path. Without loss of generality, here we assume that the resource usage on an arc is never larger than the resource storage capacity Γ, since one can simply remove such arcs from G_b if this is not the case, and use Γ as a large enough number to relax the respective constraint for an arc $(i,j) \in A_b$, if the arc is not traveled (i.e., $y_{ij} = 0$)). Clearly, $\mathcal{P}_b$ becomes a nonlinear binary program when a nonlinear resource function is considered for the fast charging (i.e., when ρ_{ij} is a nonlinear function for an arc (i,j) that represent parking in the depot. The constraint (10) sets the resource level at the origin. Finally, (11) - (12) indicates the variable domain restrictions.

Clearly, solving $\mathcal{P}_b$, $b \in B$, is not a trivial task, even when one considers a linear resource function. However, having an efficient algorithm to achieve this is critical for the overall efficiency of the CG procedure to solve large-size instances. For that purpose we develop a dynamic programming algorithm (DP) that generates such schedules by selecting trips one after another to form an ordered list of trips to be operated by a given bus type and can find "approximate" solutions of the GRSP instances on the pricing graphs. In the following, we first formally present the DP by defining its states and the value function and then discuss the practical benefits of it to efficiently solve the pricing problem by discussing the trade-offs between the computational effort and the approximation quality.

Let Ω be the set of locations that includes the start node $\boldsymbol{o}$, exit node $\boldsymbol{d}$ and the last bus stops of each trip $t \in T$. We also define a discrete set of time points Θ that includes all the trip end times (time to reach

the final bus stop) for all the trips in T, and two special time points $\theta_{\boldsymbol{o}}$ and $\theta_{\boldsymbol{d}}$ that marks the beginning and stopping times of the PT operations, i.e., $\Theta = \{\theta_{d_t} : t \in T\} \cup \{\theta_{\boldsymbol{o}}, \theta_{\boldsymbol{d}}\}$. Let $\Psi = \{\psi_0, \ldots, \psi_n\}$ be a discrete set of SOC levels, where we have $\psi_0 = 0$, $\psi_n = 1$ and $\psi_{i+1} - \psi_i = \Delta$ for all $i = 0, \ldots, n-1$. We call the parameter Δ as the *energy resolution*.

The set of states for the DP algorithm to solve the GRSP on a pricing graph G_b is denoted by W and state $w \in W$ is characterized by a three tuple $\langle \lambda_w, \theta_w, \psi_w \rangle$, representing an EB of type b to be located at $\lambda_w \in \Omega$, at time $\theta_w \in \Theta$, with a SOC $\psi_w \in \Psi$. Let T_w be the set of trips that an EB of type b can execute next when it is in a state $w \in W$. We define ψ_{wt} as the largest SOC level in Ψ that is closest to the SOC of an EB of type b after executing the trip t when it is in a state $w \in W$. The total cost of the energy to be used by an EB of type b to first travel the transition path from λ_w to the first stop of a trip $t \in T_w$ and then complete the trip t is denoted by c_{wt}.

At a state $w \in W$, the set of plausible actions is denoted by $\mathcal{A}_w$. The action set $\mathcal{A}_w$ includes a transfer action a_t for each trip $t \in T_w$ and an exit action a_e to represent the end of the schedule. For a transfer action $a_t \in \mathcal{A}$, the cost is defined as $c_{a_t} = c_{wt} - u_t$ and the cost of the exit action c_{a_e}, is simply the energy cost of the exit path $\bar{p}_w$ from λ_w to the closest depot. Taking a transfer action $a_t \in \mathcal{A}$, a state w transitions to the state $w_{a_t} = \langle d_t, \theta_{d_t}, \psi_{wt} \rangle$. On the other hand, taking the exit action a_e, a state w transitions to the *final state* $w_{\boldsymbol{d}} = \langle \boldsymbol{d}, \theta_{\boldsymbol{d}}, \psi_0 \rangle$. The value of a state $w \in W$ is determined by the value function $V : W \to \mathbb{R}$, which is defined as follows.

$$V(w) = \begin{cases} 0, \text{ if } w = w_{\boldsymbol{d}} \\ \min\{c_a + V(w_a) : a \in A_w\}, \text{ otherwise.} \end{cases} \tag{13}$$

The first case in (13) sets the boundary conditions and the second case indicates the Bellman equations to recursively calculate the value of the *initial state* $w_{\boldsymbol{o}} = \langle \boldsymbol{o}, \theta_{\boldsymbol{o}}, \psi_n \rangle$. The pseudo-code for the DP is presented in Algorithm 1. As indicated in Algorithm 1, for a given bus type $b \in B$ and the energy resolution Δ we first build the sets Ω, Θ, and Ψ. Next, two special states $w_{\boldsymbol{o}}$ and $w_{\boldsymbol{o}}$ are built to represent the start and ending of the schedule σ^* DP returns. The value of the initial state z^* is calculated at line 5 via the value function in a recursive way, as shown between lines 14 and 24. As indicated in (13), the value function V returns 0 for the final state $w_{\boldsymbol{b}}$ and for the other states $w \in W \setminus \{w_{\boldsymbol{b}}\}$ it first finds the best action at the state by comparing the best transfer action a_t^* against the exit action a_e (line 19). If the exit action is not preferable, the next trip at the state w is set to t^*, the next state to move from w is stored as w_{t^*} and the value of the state is returned as the total cost of taking the action a_{t^*} and the value of the state w_{t^*}. Otherwise, the next trip is set to null, the next state is stored as the final state $w_{\boldsymbol{o}}$ and the value of the state is returned as the cost of taking the exit action since we have $V(w_{\boldsymbol{o}})$. Once the value function calculations are finished in a recursive way, the trip list of the schedule σ^* is determined by using the stored information about the best next trips and states (lines 8-11). Finally, the bus type of the schedule σ^* is set as b, and the DP returns both the best schedule σ^* and its reduced cost ζ^*.

Let p^* be an optimal solution of the GRSP on the pricing graph G_b. Note that, if p^* stays feasible when SOC is rounded down (to the closest value in Ψ) at the end of each of its trips (as happens in DP),

Algorithm 1: DP algorithm

Input: b, Δ
Output: z_b^*, σ_b^*

$\Omega \longleftarrow \{d_t : t \in T\} \cup \{\boldsymbol{o}, \boldsymbol{d}\}$
$\Theta \longleftarrow \{\theta_{d_t} : t \in T\} \cup \{\theta_{\boldsymbol{o}}, \theta_{\boldsymbol{d}}\}$
$\Phi \longleftarrow \{0, \Delta, 2\Delta, \ldots, 1\}$
$w_{\boldsymbol{o}} = \langle \boldsymbol{o}, \theta_{\boldsymbol{o}}, 1 \rangle$, $w_{\boldsymbol{b}} = \langle \boldsymbol{b}, \theta_{\boldsymbol{b}}, 0 \rangle$
$\zeta^* = V(w_{\boldsymbol{o}})$
$\tau_{\sigma^*} \longleftarrow \emptyset$
$\bar{w} = w_{\boldsymbol{o}}$
while $NextState(\bar{w}) \neq w_{\boldsymbol{b}}$ **do**
    $t^* = NextTrip(\bar{w})$
    Add t^* to τ_{σ^*}
    $\bar{w} = NextState(\bar{w})$
$b_{\sigma^*} = b$
return ζ^*, σ^*
Procedure $V(w)$
    if $w = w_{\boldsymbol{b}}$ **then**
        return 0
    else
        $t^* = \arg\max_{t \in T_w} \left(c_{a_t} + V(w_{a_t})\right)$
        if $c_{a_t^*} + V(w_{a_t^*}) < c_{a_e}$ **then** `// if starting a new trip is more preferable then exiting`
            $NextTrip(w) = t^*$, $NextState(w) = w_{t^*}$,
            return $c_{a_t^*} + V(w_{a_t^*})$
        else
            $NextTrip(w) = null$, $NextState(w) = w_{\boldsymbol{b}}$
            return c_{a_e}

then the path p_{σ^*} found by the DP is an optimal solution of the GRSP problem on G_b. Therefore, it is not hard to see that choosing a small enough value for Δ; one can use DP to obtain GRSP solutions which can be treated as the "optimal" for all practical purposes. Also, note that the number of states in W is bounded by $|\Omega| \times |\Theta| \times \frac{1}{\Delta}$, hence, the DP algorithm has a polynomial run time for a fixed Δ. Practically this means that one can choose a reasonable small Δ value to achieve desired solution quality without significant computational difficulty. Moreover, recall that our main motivation to use DP to solve the GRSP instances is to find a schedule with a negative reduced cost if there exists any. Especially in the early iterations of the CG algorithm, where the dual costs of the trips are likely to be far from their optimal values, it is not as critical to solve the pricing problem exactly (find the schedule with the smallest reduced cost). Instead, finding reasonably high-quality solutions with less computational effort (time) can be more preferable. As such, one can also improve the overall computational efficiency of the CG procedure by first using relatively larger Δ values to find schedules with negative reduced costs and increase the resolution (use smaller Δ) gradually as needed. Indeed, we found such an approach to be quite effective to improve the computational efficiency of the CG algorithm, as we will discuss in more detail when we present the results of our numerical experiments in the following section.

2.2.2. IP solution

A branch and price algorithm can be developed to solve P by embedding the column generation approach into a branch and bound algorithm. However, a much simpler schema that takes advantage of the tight linear relaxation bounds of the path-based formulations can be used to obtain integer solutions of provably high-quality (Yildiz and Savelsbergh, 2019b,a). Our preliminary studies have shown that a small modification of the heuristic approach to solve the large integer programs with the columns generated during the solution of the linear relaxation also works well to find high-quality solutions of P within reasonable computation time.

This approach can be further enhanced by detecting and including additional columns that have not been generated by the CG algorithm, but that are helpful when searching for high-quality IP solutions. As variables are allowed to get fractional values between zero and one in the LP relaxation, LP takes advantage of that relaxation and covers a trip by multiple schedules taking fractional values whose sum is equal to one. This way, some useful schedules for the IP solutions might not have been produced during the CG iterations. Therefore, we propose a heuristic, namely IP-column-generation (ICG), to extend our basic CG iterations to obtain IP-friendly columns.

The main idea behind the ICG is to look for additional schedules when a subset of existing schedules are assumed to be operated in the solution (i.e., the respective decision variables are set to one, and the included trips are removed from the trip list). For that purpose, we do the following. After solving the LP relaxation of the problem, we select the schedule variable with the largest value, set it to one, and remove the trips that are included in the schedule and the associated constraints from the pricing problem. Then, we restart the CG procedure for the reduced problem and iteratively apply it until all the trips are removed from the pricing problem. After that, we solve P, considering all the columns that are generated so far. As we show in the following section, with such an approach, we are able to find high-quality solutions for the EBFCS that have less than 1% optimality gap for most of the instances we consider in our numerical experiments.

3. Computational experiments

This section is organized into four parts. In Section 3.1, we explain the general characteristics of the problem instances studied. Section 3.2 presents the experimental design. Implementation details are explained in Section 3.2. Finally, Section 3.4 discusses the critical computational and managerial insights we derive from our experiment results.

3.1. Problem instances

In this part, we present the details of the problem instances we consider in our experiments. In the sequence, we explain (i) the details of the PT networks studied in the problems, (ii) technical specifications and the cost parameters for the buses used in the fleets, (iii) the technical specifications of the recharging infrastructures we consider in the problem instances. For a quick reference, the main parameter values

used in our experiments are listed in Table 2.

Table 2: Main parameter values

Parameter	Unit	Value	Source
Cost of a battery pack	€/kWh	265	Nykvist and Nilsson (2015)
Cost of electricity	€/kWh	0.055	EPDK (2019)
Economic life of a bus	years	12	APTA (2013)
Battery life	years	12	Eudy and Jeffers (2017)
Salvage value of a bus	percent of purchasing price	15	Hensher (2007)
Salvage value of a battery pack	percent of purchasing price	15	Johnson et al. (2020)
Purchasing cost of a 25 m bi-articulated bus (350 kWh)	€	413,050	Consultation with IETT
Energy consumption of a 25m bi-articulated bus (350 kWh / Moderate time)	kWh/km	3	Consultation with IETT
Energy density of a battery	wh/kg	88	Majeau-Bettez et al. (2011)
Maintenance cost (EB)	€/km	0.3	Harrox and Casale (2019)
Purchasing cost of a 25 m diesel bus	€	250000	IETT auctions (`ekap.kik.gov.tr`)
Diesel consumption of a 25m bus (Moderate time)	lt/km	0.5997	Ayaz et al. (2017)
Maintenance cost (Diesel Bus)	€/km	0.84	Harrox and Casale (2019)
Purchasing cost of a 12 m bus (200 kWh)	€	250,000	Consultation with IETT
Energy consumption of a 12 m bus (200 kWh / Moderate time)	kWh/km	1.85	Gao et al. (2017)
Purchasing cost of a 12 m diesel bus	€	144,000	IETT auctions (`ekap.kik.gov.tr`)
Diesel consumption of a 12m bus (Moderate time)	lt/km	0.54	IETT (2018)
Cost of diesel	€/lt	0.67	OPET[1]

3.1.1. PT networks

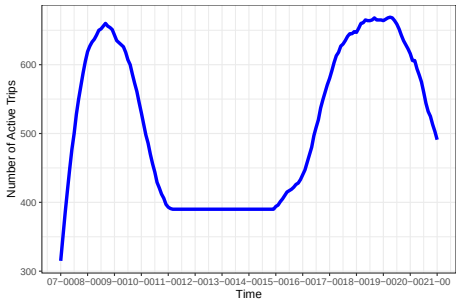
We generate our problem instances from two real-world public transit networks from Istanbul, with orthogonal properties regarding the trip frequencies, amount of road segments shared by different lines, expected number of passengers and hence the size of buses used.

BRT network - Metrobus: The BRT network, Metrobus, runs on 50.7 long dedicated lanes that pass through the most populated districts of the city. On a weekday, six lines with 6,416 trips are operated between 45 stops. Figure 2 presents the bus stop locations and the number of active trips at a given time during the day. In Figure 2a, we use different colors to illustrate the bus stops, indicating the number of trips that visit it. Green-colored stops are visited by 3,000-4,000 trips, yellow-colored stops are visited by 4,000-5,000 trips, and red-colored stops are visited by more than 5,000 trips in a day. As we see in Figure 2b, the distribution of the active trips has two peaks covering the morning and evening rush hours. In our problem instances, we consider the trips that start and end between 7 am-9 pm, which contains the bulk of the trips operated in the day. Incorporating IETT's near-term plans to enhance the service quality, the trip data we use in this study is slightly different (have a slightly larger number of trips) than the currently operated Metrobus lines.

[1]Diesel fuel price in Istanbul, on 01 September 2020, obtained from one of the main gas station chains OPET (`https://www.opet.com.tr/istanbul-akaryakit-fiyatlari`).



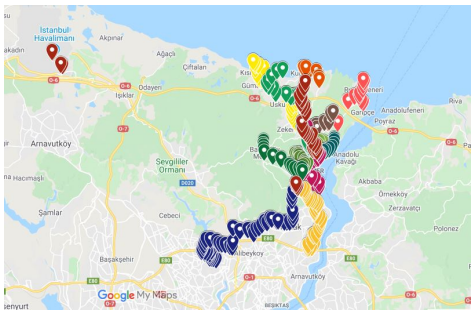
(a) Stops Visited



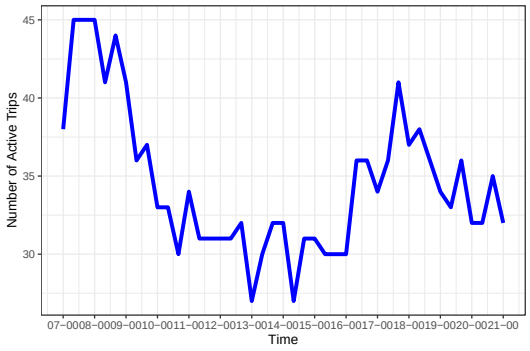
(b) Temporal distribution of trips

Figure 2: Metrobus Network

Star network - Hacıosman: Hacıosman is the terminal station of a heavily used subway line in Istanbul, and it is the hub station (also serves as the depot) for the buses carrying passengers between different districts and the subway. The road network used by the buses is a star network where the trip routes share only a small portion of the road network as shown in Figure 3a, where the stops for different lines are depicted with different colors. On weekdays, 14 lines with 846 trips are operated by 12-meter buses. The number of active trips between 7 am and 9 pm, which we consider in our instances, are shown in Figure 3.



(a) Stops visited



(b) Temporal distribution of trips

Figure 3: Hacıosman network

3.1.2. Technical specifications and cost parameters for the buses

In our problem instances, we consider 25-meter buses for the Metrobus network and 12-meter buses for the Hacıosman network to be consistent with the current practice. We solve EBFCS both for electric and diesel buses to analyze the benefits of electrification. In the sequence, we present the technical details and associated cost parameters for the electric and diesel buses we consider in our experiments.

25-meter electric buses: We consider four different EB configurations with varying battery capacities of 200, 250, 300, and 350 kWh in the Metrobus problem instances. The cost of EB battery packs are assumed to be proportional to the total energy storage capacity and taken as 265 € per kWh (Nykvist

and Nilsson, 2015). The purchasing cost of a 25 meter bi-articulated bus with 350 kWh battery size is taken as 413,050 € based on the previous analysis made by IETT.

To be consistent with the literature and the official guidelines for making the economical life analysis we take the economic life of a bus as 12 years (APTA, 2013) and the salvage value of a bus is considered to be 15% of its purchasing price (Hensher, 2007). Similarly, we take the economic life of a battery as 12 years (Eudy and Jeffers, 2017) and the salvage value of a battery pack is considered to be 15% of its purchasing price (Johnson et al., 2020).

Based on the previous analysis done by IETT, the energy consumption of a 25-meter bi-articulated bus with a 350 kWh battery is considered as 3 kWh per km for a trip operated with the moderate passenger load. As the passenger load effects the energy consumption and it differs from trip to trip (depending on the trip time), we calculate the energy consumption of each bus type for three passenger load profiles as presented in Table 3[2]. Trips between 6-9 am and 5-8 pm operate at full capacity, trips between 9-11 am, 3-5 pm and 8-10 pm operate with full seating and half standing capacity, trips in the rest of the day are operated with full seating capacity. Finally, Based on a recent analysis from a real-world use of EVs in public transit lines (Harrox and Casale, 2019), we assume that the per km maintenance cost for EBs is 0.3 €.

Table 3: Energy consumption rates for EBs on Metrobus network

Battery size	Empty weight (t)	Battery weight (t)	Time	Number of passengers	Passenger weight (t)	Total weight (t)	Consumption ($kWh.km^{-1}$)
200	22.3	2.27	Off Peak	52	3.38	27.95	2.67
			Moderate	147	9.56	34.13	2.93
			Peak	230	14.95	39.52	3.15
250	22.3	2.84	Off Peak	52	3.38	28.52	2.69
			Moderate	147	9.56	34.7	2.95
			Peak	230	14.95	40.09	3.18
300	22.3	3.41	Off Peak	52	3.38	29.09	2.72
			Moderate	147	9.56	35.26	2.98
			Peak	230	14.95	40.66	3.2
350	22.3	3.98	Off Peak	52	3.38	29.66	2.74
			Moderate	147	9.56	35.83	3
			Peak	230	14.95	41.23	3.23

25-meter diesel buses: We take the purchasing cost of a 25-meter diesel bus as 250,000 €, based on the previous auctions (`ekap.kik.gov.tr/`), and assume that the salvage value of a bus is 15% of its purchasing price (Hensher, 2007). We want to note that the purchasing costs we use in this study are based on the actual auction results for previous IETT purchases, which are significantly less than the values publicly announced by the bus manufacturers due to the several factors including bulk purchases, tax exemptions, government incentives, regional cost parameters, result in lower prices in the auctions.

The diesel consumption of a bus is considered as 0.5997 lt/km for a trip operated in a moderate time (Ayaz et al., 2017). The adjusted fuel consumption amounts for different passenger load profiles are

[2]To determine consumption rates we first calculate weights of different bus types for different number of passengers using the bus design by Göhlich et al. (2018), with the energy density of 88 $wh.kg^{-1}$ (Majeau-Bettez et al., 2011) and, by assuming that an average passenger weighs 65 kg. For 25-meter frames we consider EBs with 52 seating, 230 total passenger capacity, which are the values for the buses currently used in Metrobus lines. Considering the final bus weights, the energy consumption rates are calculated by considering 5% reduction in energy expenditure from the reference values for each 10% mass reduction (U.S. Department of Energy, 2013).

presented in Table 4[3]. Finally, per km maintenance cost for diesel busses is considered as 0.84 € (Harrox and Casale, 2019).

Table 4: 25-meter diesel bus fuel consumption rates

Time	Number of passengers	Passenger weight (t)	Consumption ($lt.km^{-1}$)
Off peak	52	3.38	0.41
Moderate	147	9.56	0.6
Peak	230	14.95	0.76

12-meter Electric buses: For 12-meter EBs we consider four configurations with 50, 100, 150 and 200 kWh battery packs. Cost of a 12-meter EB with 200 kWh is taken as 350,000 €, based on the previous analysis made by IETT. The energy consumption rates for the 12-meter EB configurations (calculated using the same procedure as explained for 25-meter buses) are presented in Table 5.

Table 5: Energy consumption rates for EBs on Hacıosman network

Battery size	Empty weight (t)	Battery weight (t)	Time	Number of passengers	Passenger weight (t)	Total weight (t)	Consumption ($kWh.km^{-1}$)
50	11.6	0.57	Off Peak	26	1.69	13.86	1.71
			Moderate	38	2.47	14.64	1.75
			Peak	103	6.7	18.86	1.99
100	11.6	1.14	Off Peak	26	1.69	14.43	1.74
			Moderate	38	2.47	15.21	1.79
			Peak	103	6.7	19.43	2.02
150	11.6	1.7	Off Peak	26	1.69	14.99	1.77
			Moderate	38	2.47	15.77	1.82
			Peak	103	6.7	20	2.06
200	11.6	2.27	Off Peak	26	1.69	15.56	1.81
			Moderate	38	2.47	16.34	1.85
			Peak	103	6.7	20.57	2.09

12-meter diesel buses: We take the purchasing cost of a 12-meter diesel bus as 144,000 €, based on the previous auctions (`ekap.kik.gov.tr/`). The fuel consumption of a 12-meter diesel bus is considered as 0.54 lt/km for a trip operated in a moderate demand time (IETT, 2018). The adjusted fuel consumption amounts for different passenger load profiles are presented in Table 6.

Table 6: 12-meter diesel bus fuel consumption rates

Time	Number of passengers	Passenger weight (t)	Consumption ($lt.km^{-1}$)
Off peak	26	1.69	0.52
Moderate	38	2.47	0.54
Peak	103	6.7	0.67

3.1.3. Technical specifications of the recharging infrastructures

We study five levels for the DWPT pick-up power as $\psi_w \in \{22, 40, 60, 80, 100\}$ kW. Similarly, for the fast-charging we study the following levels $\psi_f \in \{60, 90, 120, 150, 180\}$ kW. Cost of electricity per kWh is taken as 0,055 €, which is the current price for commercial usage (EPDK, 2019).

[3]The fuel consumption parameter is adjusted by reducing 0.3 liter per 100 km per 100 kg mass reduction (Redelbach et al., 2012) for different passenger load profiles as shown in the Table 4.

For the Metrobus network, five different DWPT infrastructure configurations are studied with varying coverage values starting from 0% of the network length up to 100%. While selecting the road segments to equip with DWPT, we prioritize the road segments that are visited by the higher number of trips. The details about the DWPT infrastructure configurations we study in Metrobus instances can be found in Table 7.

Table 7: Metrobus DWPT infrastructure configurations

Configuration	Network coverage (% of network length)	Network coverage (% of traveled length)
MC-0	0.00	0.00
MC-25	25.15	31.10
MC-50	50.30	59.66
MC-75	74.16	80.73
MC-100	100.00	100.00

In Hacıosman network, a large proportion of the network consists of secluded areas which are visited by very few of the buses, and obviously these parts of the network are not the proper choice for installing DWPT. Therefore, we use configurations with at most 15% infrastructure coverage which maps to 50% of travel length. The configuration details can be found in Table 8.

Table 8: Hacıosman DWPT infrastructure configurations

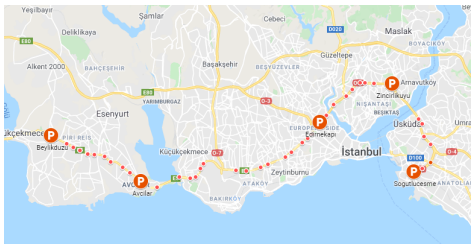
Configuration	Network coverage (% of network length)	Network coverage (% of traveled length)
HC-0	0.00	0.00
HC-2	1.82	13.27
HC-4	3.63	25.47
HC-8	8.16	37.69
HC-15	14.69	49.89

Considering the SOC levels we allow in our model, we use a piece-wise recharge function (14) to obtain the charge level increase for a given charging time λ (hour) at a depot equipped with a charger where the minimum charging time ϕ is limited to 15 minutes. The depots that are used as both parking garages and as the fast charging stations are shown in the Figure 4

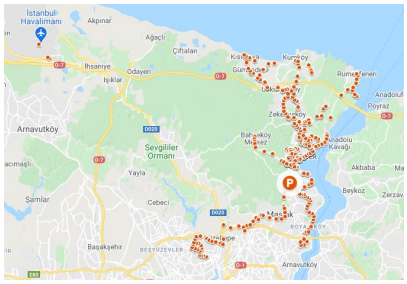
$$f(\lambda) = \begin{cases} 0, & \text{if } \lambda < 0.25 \\ \lambda \psi^F, & \text{otherwise.} \end{cases} \tag{14}$$

3.2. Experimental design

We organize our experiments in two groups, each building on the *base-case* parameter settings BC-M and BC-H, separately defined for Metrobus and Hacıosman instances. In BC-M, we consider the infrastructure configuration MC-25, fast-charging power $\psi^f = 60$kW, and DWPT pick-up power $\psi^w = 22$kW. Similarly, in BC-H, we consider the infrastructure configuration HC-4, fast-charging power $\psi^f = 60$kW, and DWPT



(a) Metrobus Network



(b) Hacıosman Network

Figure 4: Depot Locations

pick-up power $\psi^w = 22$kW.

- The first set of experiments (E1) analyzes the impact of DWPT coverage and pick-up power on the fleet composition and the total cost. For that reason, we set the fast-charging power to its base-case value and generate 50 instances, by considering all the combinations of recharging infrastructures listed in tables 7 and 8, and the DWPT pick-up power levels $\psi_w \in \{22, 40, 60, 80, 100\}$. In the remainder of the paper, E1 instances from Metrobus and Hacıosman networks are referred to as M-1 and H-1 instances.

- The second set of experiments (E2) analyzes the effect of the fast-charger power on the fleet composition and the total cost. Setting infrastructure configuration and DWPT pick-up powers to their base-case values, we generate five instances, separately for Metrobus and Hacıosman networks, and study the fast charging power levels of $\psi_f \in \{60, 90, 120, 150, 180\}$. In the remainder of the paper, E2 instances from Metrobus and Hacıosman networks are referred to as M-2 and H-2 instances.

For each network we also solve the scheduling problem separately the Diesel buses, with the specifications indicated in Section 3.1.

3.3. Implementation

In our preliminary experiments we observed that despite the high efficiency of the DP algorithm to solve the pricing problems, due to the high number of trips and the need to go through an extensive number of CG iterations solving the linear relaxation of the mathematical model P for the Metrobus instances can take quite long. For practical reasons to complete our experiments in a reasonable amount of time and taking advantage of the special structure of the Metrobus instances, we devised a decomposition approach that can provide LP relaxation solutions that are almost the same as the optimal solution of the whole problem in less than three hours.

As one can see in Figure 2, at any given time, the number of simultaneous trips in the Metrobus instances is quite high (above 650 during the rush hours and more than 375 throughout the day). Noting that the same schedule cannot cover two simultaneous trips, we divide the trip set into 20 homogeneous sub-groups, solve each of the resulting sub-problems separately, and merge the sub-problem solutions to

obtain a solution for the whole problem. Implying that the suggested decomposition approach does not significantly impact the solution quality, we observed that the linear relaxation solution we obtain with this decomposition approach, for the BC-M instance, is only 0.9% worse than the optimal linear relaxation solution of the entire problem. Considering the trade off between the solution time and quality, we use this decomposition approach to solve the Metrobus instances in our experiments.

We start the CG procedure by considering 5 kWh energy intervals for the Metrobus instances. This maps to $\Delta \in \{0.031, 0.025, 0.021, 0.018\}$ for battery sizes $\beta \in \{200, 250, 300, 350\}$. When CG stops without finding a schedule with these resolutions, we restart it with 1 kWh intervals, i.e., $\Delta \in \{0.0062, 0.0050, 0.0042, 0.0036\}$. Similarly, we start solving the Hacıosman instances with 2 kWh energy intervals and reduce the interval widths to 1 kWh when no new schedules can be found with 2 kWh resolution.

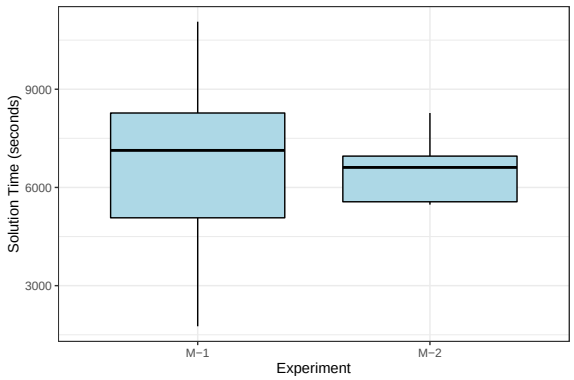
We implemented our solution approach in Java. All experiments were run on a 64-bit Linux-operated workstation with an Intel Xeon Gold 6134 processor at 3.20 GHz and 96 GB of RAM. We used CPLEX 12.10 for solving LPs and IPs. The time limit is set to three hours for solving the IP (after the CG procedure is stopped) for Hacıosman instances and two hours for Metrobus instances.

3.4. Analysis

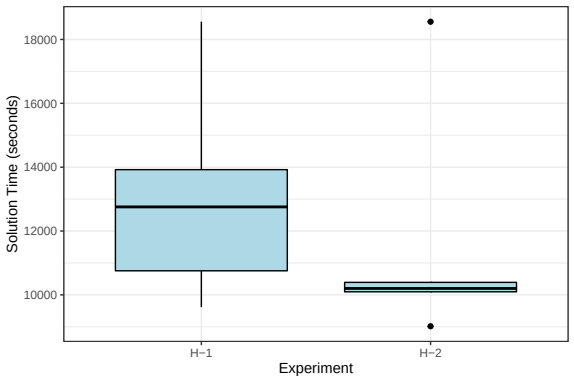
3.4.1. Computational performance

Before analyzing the experiment results from a managerial perspective, we first investigate the computational performance of the suggested algorithms and assess the viability of using them to solve real-life problems.

Detailed solution statistics for Metrobus and Hacıosman instances are presented in Tables 10 and 11, in Appendix B. However, the critical information about the computational efficiency of the CG approach is illustrated in Figures 5, 7 and 6, which illustrate the distribution of the solution times, number of column generation iterations, and the integrality gaps for all the problem instances we study in our computational experiments. In Figure 5, we observe that almost all of the problem instances have been solved in less than two hour CPU time, where the average solution time is 3.47 hours for Metrobus instances and 1.71 hours for Hacıosman instances. Looking at the number of CG iterations in Figure 6, we can see the DP approach's critical role in solving pricing problems efficiently to achieve such a remarkable run time performance. As expected, we also see that the number of CG iterations is much higher in the Metrobus instances (with almost eight times more trips than that of Hacıosman instances), revealing the benefit of the decomposition approach we consider to solve these instances in a reasonable amount of time. Finally, the integrality gaps which are calculated by $\frac{z_{IP}-z_{LP}}{z_{IP}} \times 100$ where z_{IP} and z_{LP} denote the objective values found by IP heuristic and LP relaxation respectively depicted in Figure 7 show that the IP solution procedure we describe in Section 2.2.2 can indeed produce high-quality solutions that can be confidently used to derive important managerial insights as we discuss in the next section.

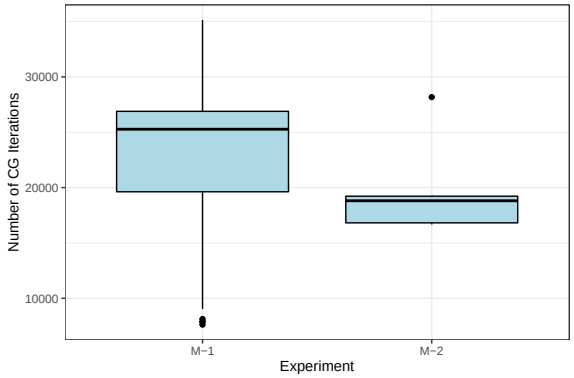


(a) Metrobus experiments

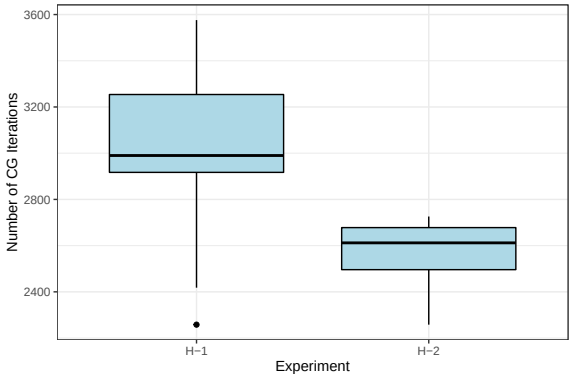


(b) Hacıosman experiments

Figure 5: Run time

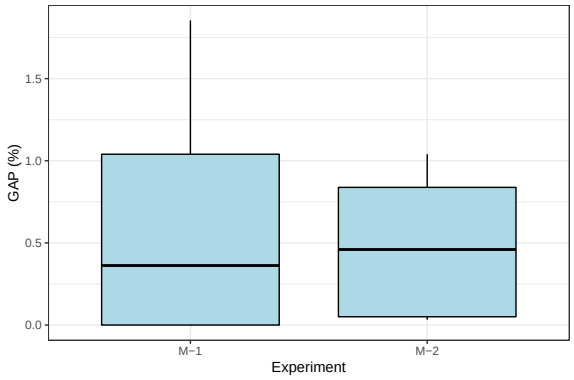


(a) Metrobus experiments

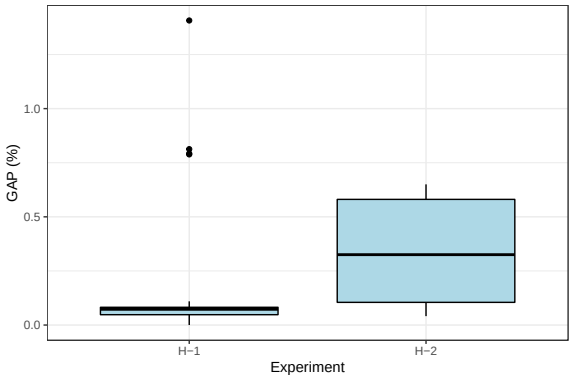


(b) Hacıosman experiments

Figure 6: Number of CG iterations



(a) Metrobus experiments



(b) Hacıosman experiments

Figure 7: Optimality gap

3.4.2. Benefits of electrification

The most striking result we observe from the experiment results (reported in Tables 10 and 11) is the cost advantage of the EB fleets over the diesel bus fleets, for both the Metrobus and Hacıosman networks. To make the comparison easier, in Table 9 we summarize the critical solution statistics for the EB and diesel bus fleet compositions and resulting cost structures, where for the EB fleet, we consider the base case settings for the fast charging ($\psi_f = 60$ kWh) and no DWPT infrastructure (i.e., configurations MC-0 and HC-0).

Table 9: Optimal fleet composition for electric and diesel buses

	Metrobus network		Hacıosman network	
	Electric bus fleet	Diesel bus fleet	Electric bus fleet	Diesel bus fleet
Number of buses used (200 kWh)	18		0	
Number of buses used (250 kWh)	28		2	
Number of buses used (300 kWh)	127		9	
Number of buses used (350 kWh)	772		43	
Number of buses used (Diesel)		740		45
Total number of buses used	945	740	54	45
Procurement cost (M€)	403.61	190.59	15.92	6.01
Electricity cost (M€)	123.79		4.32	
Fuel cost (M€)		306.08		17.66
Maintenance cost (M€)	222.36	613.26	12.28	34.38
Total cost (M€)	749.76	1109.93	32.52	58.06
Saving by electrification (%)	32.44		43.99	
Fleet size change after electrification (%)	+27.03		+20.00	

As we observe in Table 9, although electrification increases the number of buses needed (from 740 to 945 in the Metrobus network and from 45 to 54 in the Hacıosman network), it still reduces the total cost incurred. Despite the higher purchase cost of the EBs, the main drivers of the cost reduction are the well-known energy and maintenance costs advantages of the electric power trains. Clearly, the ratios between the price of an electric bus and a diesel bus, between the price of electricity and the price of fuel, between the maintenance costs of electric and diesel buses, and between the consumption levels of electric and diesel buses are the critical parameters determining the least cost option, and they may change over the economic life of the bus fleets (12 years in our analysis). However, the large margin between the total costs of the two alternatives indicates that the cost advantage of the EB fleets is highly robust and likely to be maintained, if not enhanced, under almost all the plausible scenarios about the future realizations of these cost parameters. We see that an EB bus fleet can reduce the total cost by more that 30% for the Metrobus and more than 40% for the Hacıosman networks. Keeping other factors constant, a diesel bus fleet can be the optimal choice for both networks only if the ratio of electricity price to fuel price increases by 592.25% or the ratio of the maintenance cost of EB to the maintenance cost of a diesel bus increases by 207.98%.

As an interesting and somewhat counterintuitive result, we also observe that the saving obtained through the electrification of the Hacıosman network is higher than that of Metrobus network. Considering that EBs have higher procurement costs than their combustion engine counterparts and their main

advantage is the low operational costs (energy and maintenance) one would naturally expect that the benefits of electrification would be higher in the Metrobus network with higher vehicle utilization rates. However, a more careful thinking reveals that, beyond a threshold, higher utilization can hurt the cost advantages of EBs as a larger fleet may be needed to compensate for the loss of operational time due to the recharging. Indeed, we see in Table 9 that the size of the EB fleet is 27% larger than the corresponding diesel bus fleet in the Metrobus network, whereas this figure is 20% in the Hacıosman network since the trip frequencies are higher and hence the time for recharging is more limited in the former. Following up on this observation, in the next subsection, we investigate the role of the DWPT to improve the operational availability of EBs and reducing their procurement costs by reducing the size of the batteries needed.

We want to underline that in this study, we approach the EB fleet composition problem from a strategic perspective and develop a deterministic model to study it. Considering the inherent limitations of such models, one natural question that comes to mind is how robust are the schedules produced by the deterministic model against the stochastic changes in the energy consumption rates on the road segments. To get an idea about how much effort and backup capacity (extra buses) would be needed at the operational level to ensure an uninterrupted service, we conduct a set of simulation experiments as described in the following. Assuming that the energy consumptions are normally distributed with means equal to the parameter values we use in our model and investigating the coefficients of variation $\upsilon \in \{0.01, 0.05, 0.1\}$, we sample 100 scenarios (realizations of energy consumptions in each road segment in each trip). For each scenario, we check whether schedules stay feasible with the randomly drawn energy consumption rates. If in a scenario an EB cannot complete a trip t in its schedule σ (due to the increased energy consumption in previous trips) starting from t we remove one or more successive trips from σ (get them executed by a backup vehicle), and use the saved time to recharge the EB and reposition it (if necessary) to continue its schedule after the skipped trip(s). Figure 8 presents the results of these experiments with the box plots showing the percentages of trips that need to be rescheduled for various values of coefficient of variation (υ). The figure presents only the results for the Metrobus network, as all Hacıosman schedules stayed feasible in all sampled scenarios, even for $\upsilon = 0.1$. Since the frequencies of trips are much lower in Hacıosman lines and the EBs have longer waiting times in the depots, we see that the fluctuations in energy consumptions are easily tolerated.

As we can see in Figure 8, even with the naive rescheduling approach we consider in the simulations, the percentage of trips that need to be skipped is quite small, indicating the robustness of the deterministic solutions even for the bustling Metrobus network. Obviously, the robustness of the deterministic solutions degrades as the variance in the energy consumption levels increases, indicating that in the case of high variances in energy use, extra measures, such as adding a safety buffer to the minimum allowed SOC (ϵ^{min}), should be considered when solving EBFCS.

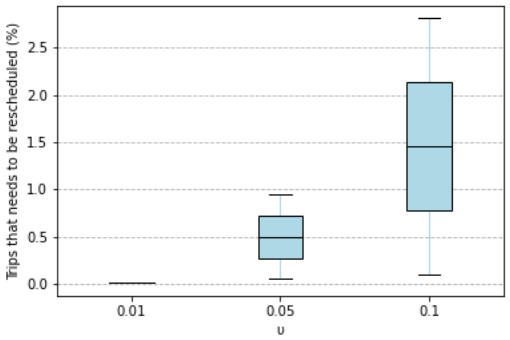


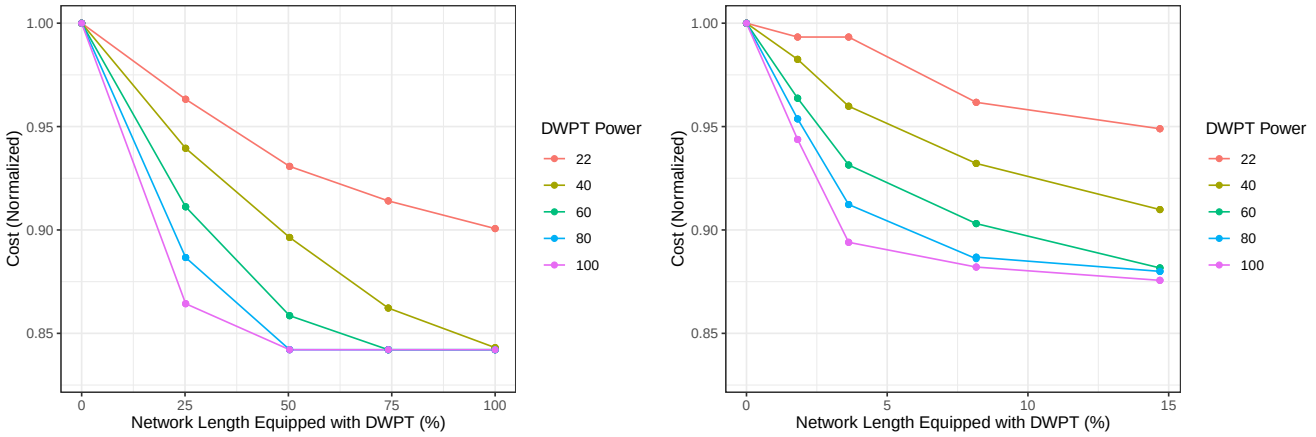
Figure 8: Metrobus network simulation results with stochastic energy consumptions

3.4.3. Benefits of DWPT

Results of M-1 and H-1 experiments reveal interesting results on the potential benefit of DWPT to enhance the cost advantages of the EB fleets against their combustion engine counterparts.

The changes in the total costs for the varying levels of infrastructure deployment and pick-up power levels are presented in Figure 9, for the Metrobus and Hacıosman networks. In the graphs, we report the normalized costs against the total cost of the problem instance with no DWPT infrastructure (configurations MC-0 and HC-0). As we can observe from these figures, DWPT can provide significant cost savings (more than 118M € for the Metrobus Network and 4.04 € for the Hacıosman Network). Here we want to underline that these calculations do not consider the cost of installing the DWPT infrastructure. Thus, the actual decision to set up such an infrastructure should be based on comparing the total savings against the cost of making such an investment. In that regard, we see that the sheer size of the Metrobus Network may justify deploying DWPT in a significant portion of the road network (i.e., 25-50%) while a smaller DWPT coverage might be a better option (from the cost perspective) for the Hacıosman Network where the number of trips and the amount of the road segments shared by different trips is much smaller. Another important insight one can derive from these results is the critical importance of the DWPT pick-up power, especially when the DWPT covered road segments are not as much. Such a result gives a clear guidance for the developers of the technology to make it more appealing to use in practice.

Taking a closer look at the impact of the DWPT on fleet size and structure reveals that besides the total cost, the technology may have other significant benefits. In Figure 10, we depict the EB fleet compositions for varying DWPT infrastructures, where the experiment labels in the horizontal axis indicate the respective DWPT configuration and pick-up power (e.g., MC-0:22 indicates the Metrobus problem instance with configuration MC-0 and pick-up power 22kW). As we can see from the figures, by increasing the EBs' operational availability, DWPT can significantly reduce the required number of busses in the EB fleets (from 945 to 740 in Metrobus Network and from 54 to 45 in Hacıosman Network). Moreover, the total required battery capacity can be reduced by 53.6% and 69.8% in Metrobus and Hacıosman fleets. Considering the negative environmental impacts of manufacturing EBs and their batteries, it is not hard to see that such huge decreases in the number of EBs and the battery sizes can

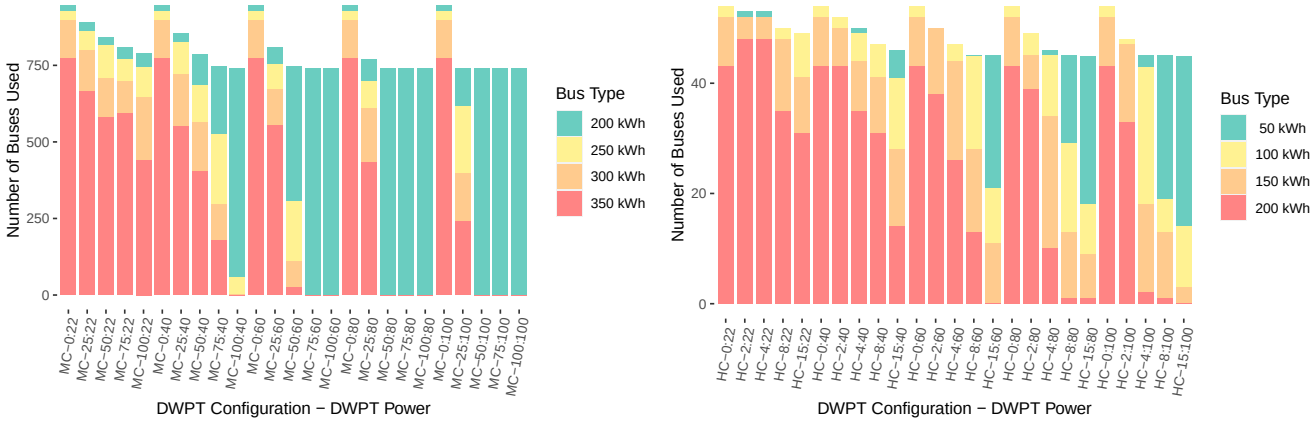


(a) Metrobus network

(b) Hacıosman network

Figure 9: Cost benefits of DWPT

provide significant environmental benefits. Besides, reducing the required number of EBs and the battery capacities means smaller procurement costs (27.3% and 28.27% less for Metrobus and Hacıosman EB fleets) which reduces the needed funds for the initial investment. The resulting financial benefits can obviously play an important role in easing the electrification of the public transportation networks.



(a) Metrobus network

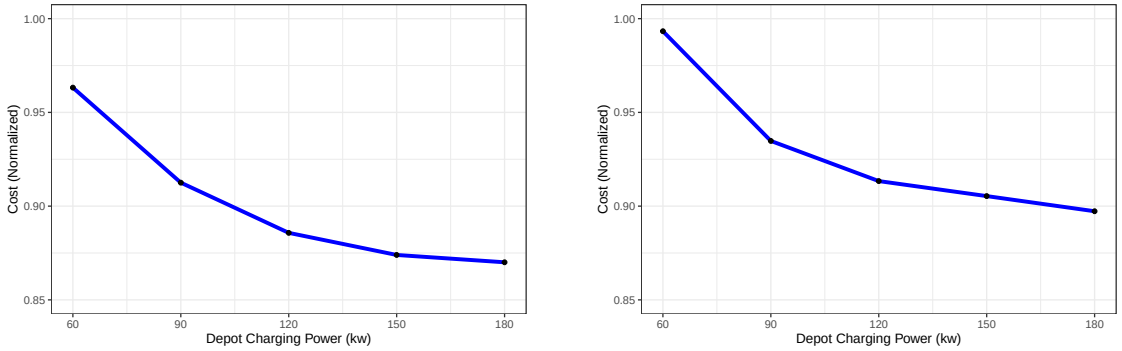
(b) Hacıosman network

Figure 10: EB fleet compositions for different DWPT infrastructures

Finally, as a side benefit of the reduced battery sizes, hence the decreased bus weights, DWPT can reduce the total energy consumption of EBs. Indeed, in Table 10 we observe that DWPT can reduce the total electricity cost for the Metrobus Network by 4.6M €, which indicates an energy saving of more than 83.6GWh. Considering 0.45 kg of CO2 emissions per kWh (U.S. Energy Information Administration). Such a saving would result in 37.6M tons of less CO2 emissions.

3.4.4. Benefits of fast charging

Clearly, fast-charging is a critical capability to enable electric transportation in public transportation networks. Results of M-2 and H-2 experiments reveal important benefits of reducing the recharging times (increasing the fast charging power). Figure 11 presents the total cost procurement and operational costs of EB fleets, for Metrobus and Hacıosman networks, for various recharging power levels. As expected, we see that increasing the fast charging power can provide significant cost reductions. However, as an interesting insight (both for technology developers and the PT agencies to decide among alternatives), the benefit of higher power fast chargers is substantial until a threshold (i.e., 120kW for both networks) beyond which marginal benefit of higher charging powers drops drastically.



(a) Metrobus Network (b) Hacıosman Network

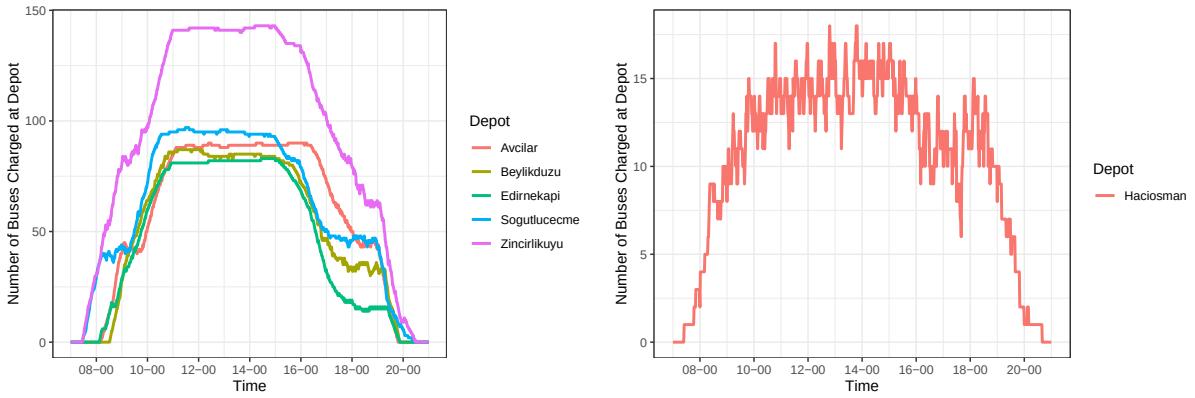
Figure 11: Reduction in the Total Cost with the Increased Recharging Power

Unlike the benefits of improving the DWPT capabilities, we observe in Figure 11, the benefits of higher power chargers are slightly more pronounced in Metrobus Network than Hacıosman Network. This is not surprising since the operational availability of EBs is more critical in the former, as discussed before, and the main contribution of higher power fast chargers is to improve the operational availability of the EBs by reducing the recharging times.

3.4.5. Spatial and temporal distribution of fast chargers

In this study, based on our consultations with IETT, we assume that the depots are equipped with enough chargers to serve EBs at any time. As such, one indirect output of our model is to show the number of fast-chargers needed in each depot, which can be inferred by examining the spatial and temporal distribution of the charging activities in the optimal solutions of EBFCS . In Figure 12, we present the number of EBs plugged-in for recharge at a given time during the day, separately for each depot, in the base-case solution. As we can see from the figure, in both networks EBs are mostly charged during the off-peak passenger demand hours (11 am - 4 pm). Although such a temporal concentration of fast-charging activities increases the number of fast-chargers needed in the system, it is arguably the best option since any other alternative would inevitably increase the number of EBs whose procurement costs are much higher than the procurement costs of the fast chargers. As an interesting insight, we also see that conducting most of the day-time charging between the 11 am - 4 pm interval also fits well to the

city's overall electricity demand, which has the lowest morning time values between 11 am - 4 pm (EPDK, 2020).



(a) Metrobus Network

(b) Hacıosman Network

Figure 12: Number of buses being charged at the depots

For the spatial distribution of the fast-charging activities in the Metrobus network, we see that, even though our model does not explicitly consider distributing them evenly among the five depots, the resulting solutions present a reasonably balanced distribution. Although the concentration in the Zincirlikuyu depot is higher compared to the rest, its central location explains this result (see Figure 4a). Clearly, for the Hacıosman network with a single depot, the spatial distribution is not an issue.

4. Final remarks

In this paper, we introduce the Electric Bus Fleet Composition and Scheduling Problem to the literature and investigate the economic viability and potential benefits of using EBs in public transit networks. In order to develop an efficient solution methodology for this challenging problem, we model it using a basic set partitioning formulation and develop a column generation approach for its solution. With the help of a novel dynamic programming approach for solving the pricing problem in an efficient way, the suggested methodology can provide provably high-quality solutions (i.e., with less than 2% optimality gaps in our numerical studies) for the large size real-world problem instances we study in this paper.

To test the efficacy of our solution methodology and derive important managerial insights, we conducted extensive numerical experiments. We examined the combined effect of infrastructure coverage and DWPT pick-up power and the effect of fast charger power on the potential benefits and viability of electrification of public transit networks. Aiming to base our analysis on a more comprehensive set of experiments, we study problem instances from two real-world public transit networks, with orthogonal properties regarding the trip frequencies, amount of road segments shared by different lines, expected number of passengers, and hence the size of buses used. Different than the existing studies, which compare the life-cycle costs of EBs with their combustion engine counterparts typically from an individual vehicle perspective, our study takes a system-wide perspective and considers the whole fleet composition and

real-world operational conditions. Thus, our results provide broader and more realistic insights regarding the potential benefits of electrification and the critical roles of the new recharging technologies to extend it further. In particular, our results show that, even though the fleet sizes may increase when replacing combustion engine buses with EBs, electrification of PT systems can still reduce the cost of a fleet significantly according to the current market parameters. Our results also indicate that the capital investments and operational costs can be reduced even further with a properly designed DWPT infrastructure which can significantly reduce the number of required EBs and the size of their batteries.

With the unique system wide perspective, our results also provide important insights for the technology developers to assess which performance levels are critical to achieve to make the technology more appealing in the practice. Similarly, PT authorities can benefit significantly from these results to make more informed cost benefit analyses of alternative technologies and infrastructure configurations.

In this study, we approached to the EB fleet composition problem from a strategic perspective and developed a deterministic model to study it. Clearly, in the operational level stochastic energy consumption, passenger numbers and boarding times, charging scheduling and crew scheduling issues should be considered for the real time management of the system, which points to an interesting direction for future studies. Also, as another limitation, this study does not consider possibility of future changes in the PT networks (i.e., changes in the routes, trip frequencies, speed profiles. etc.), while deciding the EB fleet composition. Therefore, it will be important for future studies to extend the basic approaches presented in this study to develop a multi period planning approach. Finally, we would like to conclude by pointing out that the model we problem definition and the respective model we present in this study disregard the fact that dismissing all the existing combustion engine buses at once to replace them with EBs is not practical, especially for large networks. As such, new approaches are needed to study optimal transition plans from diesel buses to EBs, which opens up an interesting new research direction we plan to pursue in our future studies.

Acknowledgments

The second author has been supported from Bilim Akademisi - The Science Academy, Turkey under the BAGEP program. This work would not have been possible without the assistance of the IETT Technology Development Unit. We thank them not only for providing us with real-life data, but also for the many informative and insightful discussions.

References

Optimizing battery electric bus transit vehicle scheduling with battery exchanging: Model and case study. *Procedia - Social and Behavioral Sciences*, 96:2725–2736, 2013. ISSN 1877-0428. doi: https://doi.org/10.1016/j.sbspro.2013.08.306. URL `https://www.sciencedirect.com/science/article/pii/S1877042813024324`. Intelligent and Integrated Sustainable Multimodal Transportation Sys-

tems Proceedings from the 13th COTA International Conference of Transportation Professionals (CICTP2013).

Alternative Fuels Data Center. Fuel properties comparison, 2014. URL https://afdc.energy.gov/fuels/fuel_comparison_chart.pdf.

Kun An. Battery electric bus infrastructure planning under demand uncertainty. *Transportation Research Part C: Emerging Technologies*, 111:572–587, 2020.

Yash P Aneja, Vijay Aggarwal, and Kunhiraman PK Nair. Shortest chain subject to side constraints. *Networks*, 13(2):295–302, 1983.

APTA. Standard bus procurement request for proposal (rfp). Technical report, American Public Transportation Association (APTA), May 2013. URL https://www.apta.com/researchtechnical-resources/standards/procurement/apta-bts-bpg-gl-001-13.

Ramazan Ayaz, İsmail Nakir, Ali Durusu, Hakan Akca, and Mugdesem Tanrioven. A comparison of metrobus system and trolleybus system considering energy costs and co2 emission: A case study for istanbul. 28, 2017.

Alan A Bertossi, Paolo Carraresi, and Giorgio Gallo. On some matching problems arising in vehicle scheduling models. *Networks*, 17(3):271–281, 1987.

Zicheng Bi, Lingjun Song, Robert De Kleine, Chunting Chris Mi, and Gregory A Keoleian. Plug-in vs. wireless charging: Life cycle energy and greenhouse gas emissions for an electric bus system. *Applied Energy*, 146:11–19, 2015.

Zicheng Bi, Robert De Kleine, and Gregory A Keoleian. Integrated life cycle assessment and life cycle cost model for comparing plug-in versus wireless charging for an electric bus system. *Journal of Industrial Ecology*, 21(2):344–355, 2017.

Nicolás Cabrera, Andrés L Medaglia, Leonardo Lozano, and Daniel Duque. An exact bidirectional pulse algorithm for the constrained shortest path. *Networks*, 76(2):128–146, 2020.

Avishai Ceder and Nigel HM Wilson. Bus network design. *Transportation Research Part B: Methodological*, 20(4):331–344, 1986.

Zhibin Chen, Wei Liu, and Yafeng Yin. Deployment of stationary and dynamic charging infrastructure for electric vehicles along traffic corridors. *Transportation Research Part C: Emerging Technologies*, 77: 185–206, 2017.

Qian Dai, Tao Cai, Shanxu Duan, and Feng Zhao. Stochastic modeling and forecasting of load demand for electric bus battery-swap station. *IEEE Transactions on Power Delivery*, 29(4):1909–1917, 2014.

Guy Desaulniers, June Lavigne, and Francois Soumis. Multi-depot vehicle scheduling problems with time windows and waiting costs. *European Journal of Operational Research*, 111(3):479–494, 1998.

Lucie Desfontaines and Guy Desaulniers. Multiple depot vehicle scheduling with controlled trip shifting. *Transportation Research Part B: Methodological*, 113:34–53, 2018.

Luigi Di Puglia Pugliese and Francesca Guerriero. A survey of resource constrained shortest path problems: Exact solution approaches. *Networks*, 62(3):183–200, 2013.

Irina Dumitrescu and Natashia Boland. Improved preprocessing, labeling and scaling algorithms for the weight-constrained shortest path problem. *Networks: An International Journal*, 42(3):135–153, 2003.

EPDK. 01/01/2020 tarihinden itibaren geçerli elektrik tarife tabloları hakkında, 2019. URL `http://epdk.gov.tr/Detay/Icerik/3-23448/01012020-tarihinden-itibaren-gecerli-elektrik-t`.

EPDK. Elektrik piyasasi sektor raporu, November 2020. URL `https://www.epdk.gov.tr/Detay/Icerik/3-0-23/elektrikaylik-sektor-raporlar`.

Tomislav Erdelić and Tonči Carić. A survey on the electric vehicle routing problem: variants and solution approaches. *Journal of Advanced Transportation*, 2019, 2019.

Leslie Eudy and Matthew Jeffers. Foothill transit battery electric bus demonstration results: Second report. Technical Report NREL/TP-5400-67698, National Renewable Energy Lab.(NREL), Golden, CO (United States), 2017.

Micah Fuller. Wireless charging in california: Range, recharge, and vehicle electrification. *Transportation Research Part C: Emerging Technologies*, 67:343–356, 2016.

Zhiming Gao, Zhenhong Lin, Tim J LaClair, Changzheng Liu, Jan-Mou Li, Alicia K Birky, and Jacob Ward. Battery capacity and recharging needs for electric buses in city transit service. *Energy*, 122: 588–600, 2017.

Globe Newswire. Electric bus market to grow significantly at 26.1% of cagr by 2026, March 2020. URL `https://www.globenewswire.com/news-release/2020/03/12/1999947/0/en/Electric-Bus-Market-to-Grow-Significantly-at-26-1-of-CAGR-by-2026.html`.

Dietmar Göhlich, Tu-Anh Fay, Dominic Jefferies, Enrico Lauth, Alexander Kunith, and Xudong Zhang. Design of urban electric bus systems. *Design Science*, 4, 2018.

Pablo C Guedes and Denis Borenstein. Column generation based heuristic framework for the multiple-depot vehicle type scheduling problem. *Computers & Industrial Engineering*, 90:361–370, 2015.

Pablo C Guedes and Denis Borenstein. Real-time multi-depot vehicle type rescheduling problem. *Transportation Research Part B: Methodological*, 108:217–234, 2018.

Valérie Guihaire and Jin-Kao Hao. Transit network design and scheduling: A global review. *Transportation Research Part A: Policy and Practice*, 42(10):1251–1273, 2008.

James Harrox and Matthew Casale. Electric buses in america: Lessons from cities pioneering clean transportation. Technical report, U.S. Pirg Education Fund, Environment America Research and Policy Center Frontier Group, October 2019.

Stefan Helber, Justine Broihan, Young Jae Jang, Peter Hecker, and Thomas Feuerle. Location planning for dynamic wireless charging systems for electric airport passenger buses. *Energies*, 11(2):258, 2018.

David A Hensher. *Bus transport: Economics, policy and planning*. Elsevier, 2007.

O.J. Ibarra-Rojas, F. Delgado, R. Giesen, and J.C. Muñoz. Planning, operation, and control of bus transport systems: A literature review. *Transportation Research Part B: Methodological*, 77:38–75, 2015.

IETT. Stratejik plan 2018-2022, 2018. URL `https://www.iett.istanbul/webimage/files/BASKI_iett_stratejik_plan_son\%20_hali_ic(2).pdf`.

Young Jae Jang. Survey of the operation and system study on wireless charging electric vehicle systems. *Transportation Research Part C: Emerging Technologies*, 95:844–866, 2018.

Maroš Janovec and Michal Kohání. Exact approach to the electric bus fleet scheduling. *Transportation Research Procedia*, 40:1380–1387, 2019. ISSN 2352-1465. doi: https://doi.org/10.1016/j.trpro.2019.07.191. URL `https://www.sciencedirect.com/science/article/pii/S2352146519303618`. TRANSCOM 2019 13th International Scientific Conference on Sustainable, Modern and Safe Transport.

Caley Johnson, Erin Nobler, Leslie Eudy, and Matthew Jeffers. Financial analysis of battery electric transit buses. Technical Report NREL/TP-5400-74832, National Renewable Energy Lab.(NREL), Golden, CO (United States), 2020.

Jeongyong Kim, Inho Song, and Woongchul Choi. An electric bus with a battery exchange system. *Energies*, 8(7):6806–6819, 2015.

Alexander Kunith, Roman Mendelevitch, and Dietmar Goehlich. Electrification of a city bus network—an optimization model for cost-effective placing of charging infrastructure and battery sizing of fast-charging electric bus systems. *International Journal of Sustainable Transportation*, 11(10):707–720, 2017.

Siqi Li and Chunting Chris Mi. Wireless power transfer for electric vehicle applications. *IEEE journal of emerging and selected topics in power electronics*, 3(1):4–17, 2014.

Wenxiang Li, Ye Li, Haopeng Deng, and Lei Bao. Planning of electric public transport system under battery swap mode. *Sustainability*, 10(7):2528, 2018.

Zhaocai Liu and Ziqi Song. Robust planning of dynamic wireless charging infrastructure for battery electric buses. *Transportation Research Part C: Emerging Technologies*, 83:77–103, 2017.

Zhaocai Liu, Ziqi Song, and Yi He. Optimal deployment of dynamic wireless charging facilities for an electric bus system. *Transportation Research Record*, 2647(1):100–108, 2017.

Leonardo Lozano and Andrés L. Medaglia. On an exact method for the constrained shortest path problem. *Computers & Operations Research*, 40(1):378–384, 2013.

Guillaume Majeau-Bettez, Troy R Hawkins, and Anders Hammer Strømman. Life cycle environmental assessment of lithium-ion and nickel metal hydride batteries for plug-in hybrid and battery electric vehicles. *Environmental science & technology*, 45(10):4548–4554, 2011.

Kurt Mehlhorn and Mark Ziegelmann. Resource constrained shortest paths. In *European Symposium on Algorithms*, pages 326–337. Springer, 2000.

Xiaolin Mou, Daniel T Gladwin, Rui Zhao, and Hongjian Sun. Survey on magnetic resonant coupling wireless power transfer technology for electric vehicle charging. *IET Power Electronics*, 12(12):3005–3020, 2019.

Ibrahim Muter, Jean-François Cordeau, and Gilbert Laporte. A branch-and-price algorithm for the multidepot vehicle routing problem with interdepot routes. *Transportation Science*, 48(3):425–441, 2014.

B Nykvist and M Nilsson. Rapidly falling costs of battery packs for electric vehicles. nat clim chang 5: 329–332, 2015.

Neil Quarles and Kara Kockelman. Costs and benefits of electrifying and automating us bus fleets. Technical report, 2018.

Martin Redelbach, Matthias Klötzke, and Horst E Friedrich. Impact of lightweight design on energy consumption and cost effectiveness of alternative powertrain concepts. 2012.

Celso C Ribeiro and François Soumis. A column generation approach to the multiple-depot vehicle scheduling problem. *Operations research*, 42(1):41–52, 1994.

Ons Sassi and Ammar Oulamara. Electric vehicle scheduling and optimal charging problem: complexity, exact and heuristic approaches. *International Journal of Production Research*, 55(2):519–535, 2017.

Theodora-Elli Stamati and Pavol Bauer. On-road charging of electric vehicles. In *2013 IEEE transportation electrification conference and expo (ITEC)*, pages 1–8. IEEE, 2013.

Éric D Taillard. A heuristic column generation method for the heterogeneous fleet vrp. *RAIRO-Operations Research-Recherche Opérationnelle*, 33(1):1–14, 1999.

Xindi Tang, Xi Lin, and Fang He. Robust scheduling strategies of electric buses under stochastic traffic conditions. *Transportation Research Part C: Emerging Technologies*, 105:163–182, 2019.

Barrett W Thomas, Tobia Calogiuri, and Mike Hewitt. An exact bidirectional $a^\star$ approach for solving resource-constrained shortest path problems. *Networks*, 73(2):187–205, 2019.

U.S. Department of Energy. Vehicle mass impact on vehicle losses and fuel economy, 2013. URL `https://www.energy.gov/sites/prod/files/2014/03/f13/lm070_carlson_2013_o.pdf`.

U.S. Energy Information Administration.

Marcel E van Kooten Niekerk, JM van den Akker, and JA Hoogeveen. Scheduling electric vehicles. *Public Transport*, 9(1):155–176, 2017.

Hokar Yee, Sivakumar Ramakrishnan, and Ahmad Azmin Mohamad. Modelling of charge/discharge cycle of lithium ion battery system. *Journal of Quality Measurement and Analysis, JQMA*, 10(1):39–47, 2014.

Baris Yildiz and Martin Savelsbergh. Optimizing package express operations in china. *Optimization Online*, 6799, 2019a.

Baris Yildiz and Martin Savelsbergh. Provably high-quality solutions for the meal delivery routing problem. *Transportation Science*, 53(5):1372–1388, 2019b.

Guang-Jing Zhou, Dong-Fan Xie, Xiao-Mei Zhao, and Chaoru Lu. Collaborative optimization of vehicle and charging scheduling for a bus fleet mixed with electric and traditional buses. *IEEE Access*, 8: 8056–8072, 2020.

Appendix A Generating initial set of columns

As it is sufficient to have a feasible solution to start the CG procedure, we start with a solution where each trip is covered by one bus. We use a basic iterative algorithm F presented in Algorithm 2 to find the bus type that can cover the trip with the minimum battery size.

Algorithm 2: F algorithm

Input: t, B

Output: b

```
1  b* ⟵ null
2  foreach b ∈ B do
3      ϒ ⟵ β_b ε^max  ẑ ⟵ true  ϒ ⟵ ϒ − κ^b_t  foreach r ∈ R_t do
4          ϒ ⟵ min{ϒ − κ^b_tr, β_b ε^max}
5          if ϒ < β_b ε^min then
6              ẑ ⟵ false break
7      ϒ ⟵ ϒ − κ̄^b_t if ϒ < β_b ε^min then
8          ẑ ⟵ false
9      if ẑ then
10         b* ⟵ b break
11 return b*
```

The algorithm checks each battery type to cover the given trip and returns the one with the smallest size. b^* the bus type needed is initialized in line (1). The remaining charge level of a $b \in B$ type bus, Υ, is set to the highest possible level by line (3), and a control parameter to check if the battery range is exceeded is initialized in line (4). The remaining charge level is updated for traveling the start path p_t by line (5) and for each road segment $r \in R_r$ by line (7). If the SOC range is exceeded, the control parameter is altered (9), and the procedure is terminated for the current bus type (10). The remaining charge level is updated for traveling the exit path $\bar{p}_t$ by line (11), and range control is applied (12-13). If the bus can cover the trip without exceeding the SOC range, then the bus type needed is updated (15), and the iterative procedure is terminated for the rest of the bus types (16). The bus type needed is returned in line (17). Note that we assume that the bus type with the largest battery is able to complete any trip $t \in T$; the algorithm returns null otherwise.

Appendix B Detailed experiment results

Detailed results of experiments are presented in Table 10 and 11. The first two columns indicate the experiment group and the DWPT infrastructure configurations as defined in Section 3.1. Columns ψ_f and ψ_w show the fast-charger and DWPT pick-up power. The columns named as *Cost* show the total cost, procurement cost, electricity cost, and maintenance cost over 12 years horizon. The optimal bus fleet composition is shown by the *Number of Buses Used* columns by showing how many buses are used

from each type with the given battery size. *gap* column shows the percentage optimality gap which is calculated as explained in subsection 3.4.1. The number of schedules generated is shown by $\#schedules$ column. The number of CG iterations conducted and the total run time are given by columns $\#iterations$ and $time(seconds)$.

Table 10: Metrobus experiment results

Experiment	DWPT	ψ_f	ψ_w	Cost (M €)				Number of buses used				gap (%)	# schedules	# iterations	time (seconds)
				Total	Procurement	Electricity	Maintenance	(200 kWh)	(250 kWh)	(300 kWh)	(350 kWh)				
M-1	MC-0	60	22	749.76	403.61	123.79	222.36	18	28	127	772	1.85	77254	25274	7132
	MC-50	60	22	722.18	379.56	122.47	220.16	31	60	137	664	1.04	76893	28178	8274
	MC-50	60	22	697.84	356.85	121.82	219.17	25	108	128	580	0.36	84637	30816	9552
	MC-75	60	22	685.32	344.11	121.94	219.27	39	73	104	594	0.54	90123	30817	8805
	MC-100	60	22	675.29	333.54	121.98	219.77	47	99	203	441	0.72	86271	26594	7428
	MC-0	60	40	749.76	403.61	123.79	222.36	18	28	127	772	1.85	77254	25274	7132
	MC-50	60	40	704.4	361.92	122.33	220.14	29	104	170	551	0.98	79477	28891	8582
	MC-50	60	40	672.07	330.77	121.71	219.59	101	124	161	402	1.02	86131	26891	8165
	MC-75	60	40	646.47	306.78	120.61	219.08	220	229	120	177	0.32	75070	19623	5073
	MC-100	60	40	632.12	293.82	119.27	219.02	681	58	1	0	0.01	97998	35132	11062
	MC-0	60	60	749.76	403.61	123.79	222.36	18	28	127	772	1.85	77254	25274	7132
	MC-50	60	60	683.19	342.37	121.74	219.07	53	84	118	553	0.52	86013	29271	8988
	MC-50	60	60	643.7	301.68	120.92	221.1	444	195	84	26	1.06	82088	23379	7218
	MC-75	60	60	631.36	293.15	119.19	219.02	740	0	0	0	0	81853	24018	6879
	MC-100	60	60	631.36	293.15	119.19	219.02	740	0	0	0	0	30824	7620	1866
	MC-0	60	80	749.76	403.61	123.79	222.36	18	28	127	772	1.85	77254	25274	7132
	MC-50	60	80	664.8	324.25	121.53	219.02	71	87	178	433	0.34	86892	26734	8717
	MC-50	60	80	631.38	293.15	119.2	219.03	740	0	0	0	0	75967	21540	6812
	MC-75	60	80	631.36	293.15	119.19	219.02	740	0	0	0	0	32616	8131	1873
	MC-100	60	80	631.36	293.15	119.19	219.02	740	0	0	0	0	36103	9025	2327
	MC-0	60	100	749.76	403.61	123.79	222.36	18	28	127	772	1.85	77254	25274	7132
	MC-50	60	100	648.05	308.08	120.95	219.02	126	217	158	241	0.16	76911	20165	6102
	MC-50	60	100	631.36	293.15	119.19	219.02	740	0	0	0	0	31525	7876	1963
	MC-75	60	100	631.36	293.15	119.19	219.02	740	0	0	0	0	31782	7876	1760
	MC-100	60	100	631.36	293.15	119.19	219.02	740	0	0	0	0	36103	9025	2764
M-2	MC-50	60	22	722.18	379.56	122.47	220.16	31	60	137	664	1.04	76893	28178	8274
	MC-50	90	22	684.18	343.24	121.41	219.52	48	221	316	237	0.84	70149	19224	6957
	MC-50	120	22	664.1	324.13	120.93	219.04	108	216	240	216	0.46	69062	18810	6611
	MC-50	150	22	655.26	315.32	120.86	219.08	104	210	283	163	0.03	63848	16671	5562
	MC-50	180	22	652.33	312.87	120.43	219.02	235	152	261	113	0.05	64771	16816	5475
M-D	MC-0	0	0	1109.93	190.59	306.08	613.26	740				0	28960	28114	5612

Table 11: Hacıosman experiment results

Experiment	DWPT	ψ_f	ψ_w	Cost (M €)				Number of buses used				gap (%)	# schedules	# iterations	time (seconds)
				Total	Procurement	Electricity	Maintenance	(50 kWh)	(100 kWh)	(150 kWh)	(200 kWh)				
H-1	HC-0	60	22	32.52	15.92	4.32	12.28	0	2	9	43	0.07	7223	2990	10755
	HC-2	60	22	32.30	15.69	4.33	12.28	1	0	4	48	0.79	7962	3254	12494
	HC-4	60	22	32.30	16.81	4.32	12.28	1	0	4	48	1.41	6213	2258	18556
	HC-8	60	22	31.27	14.68	4.31	12.28	0	2	13	35	0.05	7283	2917	12756
	HC-15	60	22	30.86	14.28	4.29	12.28	0	8	10	31	0.05	9089	3278	14590
	HC-0	60	40	32.52	15.92	4.32	12.28	0	2	9	43	0.07	7223	2990	10755
	HC-2	60	40	31.95	15.35	4.32	12.28	0	2	7	43	0.81	8377	3291	13597
	HC-4	60	40	31.21	14.63	4.31	12.28	1	5	9	35	0.79	7693	3003	13923
	HC-8	60	40	30.31	13.73	4.30	12.28	0	6	10	31	0.09	8829	2950	13927
	HC-15	60	40	29.58	13.07	4.24	12.28	5	13	14	14	0.06	8178	2418	11712
	HC-0	60	60	32.52	15.92	4.32	12.28	0	2	9	43	0.07	7223	2990	10755
	HC-2	60	60	31.34	14.74	4.32	12.28	0	0	12	38	0.03	8774	3307	14632
	HC-4	60	60	30.29	13.71	4.30	12.28	0	3	18	26	0.03	8789	2895	13034
	HC-8	60	60	29.36	12.84	4.25	12.28	0	17	15	13	0.11	9235	2926	13125
	HC-15	60	60	28.67	12.23	4.16	12.28	24	10	11	0	0.07	8547	2921	13038
	HC-0	60	80	32.52	15.92	4.32	12.28	0	2	9	43	0.07	7223	2990	10755
	HC-2	60	80	31.01	14.42	4.31	12.28	0	4	6	39	0.04	8905	3442	14523
	HC-4	60	80	29.66	13.13	4.25	12.28	1	11	24	10	0.08	9310	2823	12605
	HC-8	60	80	28.81	12.35	4.18	12.28	16	16	12	1	0.06	8695	2811	10538
	HC-15	60	80	28.61	12.18	4.15	12.28	27	9	8	1	0.00	10029	3221	12807
	HC-0	60	100	32.52	15.92	4.32	12.28	0	2	9	43	0.07	7223	2990	10755
	HC-2	60	100	30.69	14.10	4.31	12.28	0	1	14	33	0.08	9645	3576	14828
	HC-4	60	100	29.07	12.58	4.22	12.28	2	25	16	2	0.05	8769	2844	12299
	HC-8	60	100	28.68	12.24	4.16	12.28	26	6	12	1	0.00	9643	3062	9616
	HC-15	60	100	28.47	12.06	4.14	12.28	31	11	3	0	0.00	9240	3369	10393
H-2	HC-4	60	22	32.30	16.81	4.32	12.28	1	0	4	48	1.41	6213	2258	18556
	HC-4	90	22	30.40	13.91	4.21	12.28	6	25	18	1	0.09	6952	2496	10202
	HC-4	120	22	29.70	13.19	4.23	12.28	0	26	18	3	0.09	7590	2678	10392
	HC-4	150	22	29.44	12.93	4.23	12.28	2	21	19	4	0.43	8233	2726	10096
	HC-4	180	22	29.18	12.67	4.23	12.28	3	17	21	4	0.04	8226	2612	9017
H-D	HC-0	0	0	58.06	17.66	34.38	58.06	45				0	2934	2934	249